Error Vector Magnitude Analysis of Fading SIMO Channels Relying on MRC Reception

Varghese Antony Thomas, Suman Kumar, Sheetal Kalyani, Mohammed El-Hajjar, K. Giridhar, and Lajos Hanzo, *Fellow, IEEE*

***Abstract*—We analytically characterize the data-aided error vector magnitude (EVM) performance of a single-input multiple-output (SIMO) communication system relying on maximal ratio combining (MRC) having either independent or correlated branches that are nonidentically distributed. In particular, exact closed form expressions are derived for the EVM in η-μ fading and κ-μ shadowed fading channels and these expressions are validated by simulations. The derived expressions are expressed in terms of Lauricella's function of the fourth kind $F_D^{(N)}(.)$, which can be easily computed. Furthermore, we have simplified the derived expressions for various special cases such as independent and identically distributed branches, Rayleigh fading, Nakagami-*m* fading, and κ-μ fading. Additionally, a parametric study of the EVM performance of the wireless system is presented.**

***Index Terms*—Error Vector Magnitude, maximal ratio combining, η-μ fading, κ-μ fading, SIMO.**

I. Introduction

CONFORMITY with the wireless communication performance standards is an absolute necessity, when designing communication systems. Traditional approaches of quantifying a communication system's performance includes the calculation of classic metrics such as the Bit Error Ratio (BER), the throughput and the outage probability [1]–[4]. However, an alternative metric that is becoming increasingly popular is the Error Vector Magnitude (EVM) [5].

EVM as a performance metric offers several advantages. Firstly, it facilitates the identification of the specific types of degradations encountered, in addition to their particular sources in a transmission link [5]. Some of these degradations are the Inphase-Quadrature Phase (IQ) imbalance, the Local Oscillator's (LO) phase noise, carrier leakage, nonlinearity and the LO's frequency error [6], [7]. Secondly, the EVM is a symbol-level performance metric unlike the BER, which is a bit-level performance metric. Hence, EVM is more convenient for Symbol Error Rate (SER) based scenarios where multiple modulation schemes are employed, as in adaptive modulation [8]. Thirdly, it may be employed by a communication system designer for ensuring conformity with wireless standards, because EVM-based specifications have already become a part of the Wideband Code Division Multiple Access (W-CDMA) and IEEE 802.11 family of Wireless Local Area Network (WLAN) standards [5], [8]. Fourthly, in experimental studies the channel model used is often a proprietary channel, for which no closed form expressions are available either for the BER or for the EVM. In these studies, the designer has to characterize the system by transmitting and receiving bits, where the BER calculation relying on the Monte Carlo approach has a long computation time, especially at low BERs. By contrast, the EVM can be readily evaluated by transmitting fewer symbols, as compared to the BER. Hence, characterizing the performance using EVM is preferred. However, in contrast to the classic BER formulae, the current literature does not provide closed form expressions of the EVM of several important channel scenarios. Hence provides closed-form expressions for some of these important channel scenarios and partially fills this gap in the open literature. We have now added the following text to the discussions in the introduction section (please see page 2 of the revised manuscript). Moreover, EVM is easier to employ than BER as a performance metric in systems, where the transmitter requires feedback regarding the link's performance for making choices such as which adaptive modulation mode or channel coding rate to rely on. This is because employing BER would require the received signal to go through the entire receive chain before the feedback can be generated, while computation of the EVM using the received symbols would be quicker. Thus, employing EVM would be a better choice for providing real-time feedback.

In an optimized system the major source of degradation is the channel's fading [4], [9]. However, in a realistic system a range of degradations mentioned in [5] are imposed, which would play a detrimental role. Employing EVM would help the designer identify these impairments at a glance and hence to mitigate them. Mitigating the effects of these distortions would require the EVM of the the best-case scenario, where the EVM is predominantly or purely decided by the wireless channel's fading as well as by the ubiquitous receiver-noise, and not by other impairments, such as non-linear distortions and synchronization errors, etc. Hence in this paper we aim for providing the designer with closed form expressions for

Manuscript received July 21, 2015; revised December 1 2015 and February 8, 2016; accepted February 12, 2016. The financial support of the EPSRC projects EP/Noo4558/1 and EP/L018659/1, as well as of the European Research Council's Advanced Fellow Grant under the Beam-Me-Up project and of the Royal Society's Wolfson Research Merit Award is gratefully acknowledged. V. A. Thomas and S. Kumar are co-first authors. The associate editor coordinating the review of this paper and approving it for publication was T. A. Tsiftsis.

V. A. Thomas, M. El-Hajjar, and L. Hanzo are with the School of Electronics and Computer Science, University of Southampton, Southampton SO17 1BJ, U.K. (e-mail: lh@ecs.soton.ac.uk).

S. Kumar, S. Kalyani, and K. Giridhar are with the Department of Electrical Engineering, Indian Institute of Technology Madras, Chennai 600036, India.

Color versions of one or more of the figures in this paper are available online at http://ieeexplore.ieee.org.

Digital Object Identifier 10.1109/TCOMM.2016.2530797

determining this best-case target EVM. Numerous models have been employed in the literature for simulating a wireless channel [4]. Some of these models have been used for several years, including the AWGN, Rayleigh, Rician and the Nakagami-m as well as the Nakagami-q faded channels. On the other hand, recent studies are increasingly favouring the state-of-the-art η-μ and κ-μ shadowed fading channels [10], [11], because they represent all-encompassing generalizations, with the classical channels being their special cases. For example, the η-μ distribution includes the Nakagami-q (Hoyt), the Nakagami-m, the Rayleigh and the One-Sided Gaussian distribution as special cases. The κ-μ distribution includes the Nakagami-n (Rice), the Nakagami-m, the Rayleigh, and the One-Sided Gaussian distribution as special cases. The κ-μ shadowed distribution includes κ-μ and Rician shadowed distribution as special cases. Moreover, they match the experimentally measured mobile radio propagation statistics better than the other channel models [10]. The κ-μ shadowed fading is useful for modelling the satellite links. A simplified model for κ-μ fading is the shadowed-Rician fading, which has been employed for modelling the satellite links [12]–[15].

The BER, outage probability and capacity are some commonly employed performance metrics, which have been quantified for η-μ and κ-μ shadowed fading[1] channels in [16]–[19] and in the references therein. On the other hand, there is a dearth of studies that focus on the quantification of the achievable EVM for these wireless channels. Moreover, there are no studies that characterize the EVM performance for the commonly employed wireless technique of receive antenna diversity [20]. Note that a performance analysis of maximal ratio combining based receive antenna diversity was provided in [21] for the case of the shadowed-Rician fading land mobile satellite channels. Employing multiple receive antennas provides a diversity gain [20], where the link between the transmit antenna and each receive antenna is referred to as a single branch of the Single Input Multiple Output (SIMO) channel. The fading coefficients of the different branches may be independently distributed or correlated, where the branches in these scenearios are referred to as being independent or correlated, respectively. Additionally, they may have the same or different probability distribution parameters, where the branches in these scenearios are referred to as being identically or non-identically distributed, respectively. It must be noted that there is some literature on the EVM performance of the classical AWGN and Rayleigh channels for the scenario of a single receive antenna, though these are limited to only a couple of research papers. The seminal effort was made in this direction in [22], while [23] formulates the attainable EVM in an AWGN scenario. This study was extended in [24] to the scenario of non data-aided receivers communicating over both AWGN as well as Rayleigh fading channels.

A designer can compute the expected BER for various fading channels using well established formulae from the existing literature. Thus, designers have a benchmark with which they can compare the experimental results, when using BER as a performance metric. However, there are no such equivalent theoretical formulae for EVM. Hence, through this paper we aim to provide a theoretical benchmark for the EVM performance that the designer can expect in the wireless channels.

Against this background, the novel contributions of this paper may be summarised as follows:

1) We derive exact closed form expressions for the data-aided EVM[2] performance of a SIMO wireless system employing the η-μ and κ-μ shadowed fading channels and a Maximal Ratio Combining (MRC) receiver. Our expressions are derived for independent and non identically distributed branches. These results are then validated by simulations[3].
2) We also study the effect of correlated fading channels in the above-mentioned wireless system and formulate the EVM for these scenarios.
3) The expressions derived are then further simplified for various special cases, such as independent and identically distributed branches, the Rayleigh, the Nakagami and the κ-μ fading.
4) The impact of the various channel parameters such as η, μ, κ and that of the number of receive antennas N on the EVM performance is studied along with the attainable performance limits.

Our paper is organized as follows. In Section II, we present the background necessary for understanding this study, which includes discussions on the SIMO η-μ and κ-μ shadowed channel models in Section II-A and on EVM in Section II-B. Subsequently, we present our analytical characterization of the EVM performance for a SIMO wireless system in Section III, while in Section IV we provide our simulation results. Finally, we offer our conclusions in Section V.

II. Background Information

A. SIMO η-μ and κ-μ Shadowed Channel Models

For the case of a SIMO wireless channel having N receive antennas, the channel model is as follows [4]:

$$\hat{\mathbf{y}} = \mathbf{h}s + \mathbf{n}, \tag{1}$$

where s is the transmitted symbol and

$$\begin{aligned} \hat{\mathbf{y}} &= [\hat{y}_1 \;\; \hat{y}_2 \;\; \cdots \;\; \hat{y}_N]^T \\ \mathbf{h} &= [a_1 e^{j\theta_1} \;\; a_2 e^{j\theta_2} \;\; \cdots \;\; a_N e^{j\theta_N}]^T \\ \mathbf{n} &= [n_1 \;\; n_2 \;\; \cdots \;\; n_N]^T. \end{aligned} \tag{2}$$

Here $\hat{y}_k$ is the symbol received by the k^{th} receive antenna after being subjected to the multiplicative fading of $a_k e^{j\theta_k}$ and to corruption by the additive noise of n_k. In the above discussions a_k, θ_k and n_k are random variables (RVs), whose pdf has to be experimentally characterized. Typically the noise is modelled by a zero-mean Gaussian distribution, while the phase of

[1]The probability distribution function (pdf) of the sum of the squared κ-μ shadowed random variables with independent and correlated shadowing components are derived in [11] and [16], respectively. Note that the pdf derived in [11] is a special case of the pdf derived in [16].

[2]Note that data-aided EVM refers to the EVM obtained using data-aided receivers, i.e receivers which have exact knowledge of the transmitted bits.

[3]Please note that if any other detector than the MRC is used, then the EVM analysis will change significantly.

the fading co-efficient is assumed to have a uniform distribution within $[0, 2\pi]$ [4]. However, modelling the distribution of a_k or alternatively that of $X_k \propto a_k^2$ is much more challenging due to its heavy dependence on the exact nature of the wireless channel. *Note that X_k is referred to as the fading power.*

Recently η-μ and κ-μ shadowed pdfs were proposed in [10] and [11], respectively. Mathematically, the η-μ fading power (or fading attenuation) pdf is expressed as follows for each X_k [10], [25]:

$$f_{X_k,\eta-\mu}(x) = \frac{2\sqrt{\pi}\mu_k^{\mu_k+\frac{1}{2}} h_k^{\mu_k}}{\Gamma(\mu_k) H_k^{\mu_k-\frac{1}{2}} \bar{x}_k^{\mu_k+\frac{1}{2}}} x^{\mu_k-\frac{1}{2}} e^{\frac{-2\mu_k h_k x}{\bar{x}_k}} \times I_{\mu_k-\frac{1}{2}}\left(\frac{2\mu_k H_k x}{\bar{x}_k}\right), \tag{3}$$

where the modified Bessel function of the first kind of order b is represented by $I_b(.)$ and the Gamma function is denoted by $\Gamma(.)$ [10]. Here we have $\mu_k = \frac{E^2\{X_k\}}{2\text{var}\{X_k\}}[1 + (\frac{H_k}{h_k})^2]$, where $E\{.\}$ and var$\{.\}$ denote the expectation and variance, respectively and $\bar{x}_k = E\{X_k\}$ [25]. The parameters H_k and h_k may be defined in two unique ways that correspond to two distinct fading formats, where the difference arises from the physical interpretation of the parameter η_k [10][4]. In format 1, $0 < \eta_k < \infty$ is the power ratio of the in-phase and quadrature phase components of the fading signal in each multipath cluster, while H_k and h_k are given by:

$$H_k = \frac{\eta_k^{-1} - \eta_k}{4} \text{ and } h_k = \frac{2 + \eta_k^{-1} + \eta_k}{4}. \tag{4}$$

Moreover, in format 1, the η-μ power distribution is symmetrical around $\eta_k = 1$. The second format can be obtained from the first one using the relationship of $\eta_{\text{format2}} = \frac{1-\eta_{\text{format1}}}{1+\eta_{\text{format1}}}$ [10].

On the other hand, the κ-μ shadowed power pdf is expressed as follows for each X_k [11]:

$$f_{X_k,\kappa_k-\mu_k sh}(x) = \frac{\mu_k^{\mu_k} m_k^{m_k}(1+\kappa_k)^{\mu_k} x^{\mu_k-1}}{\Gamma(\mu_k)(\bar{x}_k)^{\mu_k}(\mu_k\kappa_k + m_k)^{m_k}} \times e^{-\frac{\mu_k(1+\kappa_k)x}{\bar{x}_k}} {}_1F_1\left(m_k, \mu_k, \frac{\mu_k^2\kappa_k(1+\kappa_k)}{\mu_k\kappa_k + m_k}\frac{x}{\bar{x}_k}\right), \tag{5}$$

where $\kappa_k > 0$ denotes the ratio of the total power of the dominant components to that of the scattered waves and m_k is the shadowing parmeter. In (5), $\mu_k = \frac{E^2\{X_k\}}{var\{X_k\}}\frac{1+2\kappa_k}{(1+\kappa_k)^2}$ and $\bar{x} = E\{X_k\}$, while ${}_1F_1$ is the Kummer Hypergeometric function.

The elements a_k for $1 \le k \le N$ have two important characteristics, which are as follows [4]:

1) *Similarity:* For a particular distribution model, the coefficients a_k may or may not be identically distributed. Specifically, for the cases of the η-μ and κ-μ shadowed distributions, they may or may not all have the same $\{\eta_k, \mu_k\}$ and $\{\kappa_k, \mu_k, m_k\}$ parameters, respectively.

2) *Correlation:* For a particular distribution model, the coefficients a_k associated with $1 \le k \le N$ may or may not be correlated with each other. The level of correlation is represented by the correlation matrix as follows:

$$\mathbf{C_m} = \begin{bmatrix} \rho_{11} & \rho_{12} & \cdots & \rho_{1j} & \cdots & \rho_{1N} \\ \vdots & \vdots & \vdots & \rho_{ij} & \vdots & \vdots \\ \rho_{N1} & \rho_{N2} & \cdots & \rho_{1j} & \cdots & \rho_{NN} \end{bmatrix}, \tag{6}$$

where ρ_{ij} denote the correlation coefficient between a_i and a_j. Note that $\mathbf{C_m}$ is an identity matrix for the case of all fading magnitudes being independent.

In our study, we employ Maximal Ratio Combining (MRC) [4] detection, because its performance closely matches the performance of the optimal maximum-likelihood detection [4], while its complexity is much lower. Assuming perfect channel estimation, the received symbol y after MRC is as follows:

$$y = \frac{\mathbf{h}^H \hat{\mathbf{y}}}{\mathbf{h}^H \mathbf{h}}. \tag{7}$$

B. Error Vector Magnitude

The error vector between the transmitted complex-valued symbol $s(l) = s_I(l) + j \cdot s_Q(l)$ and the received symbol $y(l) = y_I(l) + j \cdot y_Q(l)$ is defined as $e(l) = y(l) - s(l)$. Fig. 1 shows a vectorial representation of e using the constellation diagram of the communication system. The EVM of the communication system is proportional to the root mean square value of the error signal $e(l)$. In other words, if a total of L symbols are transmitted over the wireless channel, then the EVM of the SIMO system described in Section II-A may be expressed as follows [24]:

$$EVM = \sqrt{\frac{\frac{1}{L}\sum_{l=1}^{L}|y(l) - s(l)|^2}{P_o}}, \tag{8}$$

where P_o is the average symbol power. If $s(l) \in \{S_1, S_2, \cdots S_M\}$, and if all symbols are equi-probable, then P_o may be expressed as:

$$P_o = \frac{\sum_{m=1}^{M}|S_m|^2}{M}. \tag{9}$$

III. Analytical Study of the EVM for SIMO Channels

The EVM in an AWGN SISO channel has been formulated as follows for the case of data-aided receivers [23]:

$$\text{EVM} = \sqrt{\frac{1}{SNR_{SISO}}} \text{ when } L \to \infty, \tag{10}$$

where SNR_{SISO} is the channel's signal-to-noise-ratio at the single receive antenna, L is the number of symbols transmitted over the wireless channel and M is the number of unique wireless symbols in the modulation scheme.

[4]It is important to note that the η-μ pdf well models the small-scale variations of the fading signal in a scenario of non-line-of-sight communication [10].

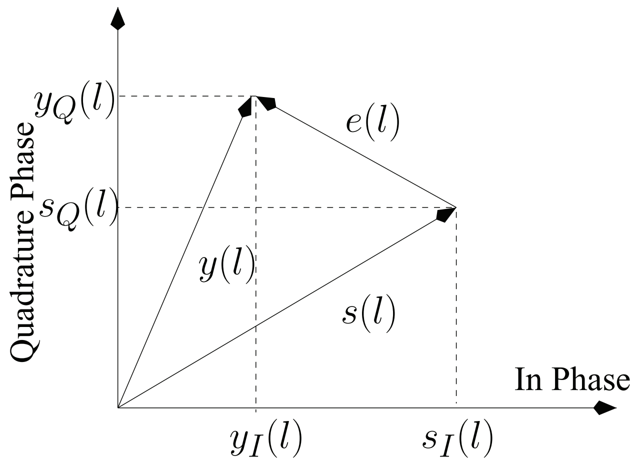

Fig. 1. Vector representation of the error between symbols s and y.

In the SIMO scenario, if we assume that the average signal to noise ratio at each receive antenna is $\gamma_i = \gamma$, then the instantaneous equivalent signal-to-noise-ratio of the overall SIMO system is [4], [24]:

$$\gamma_{inst} = \sum_{k=1}^{N} a_k^2 \gamma = N\gamma \times \frac{1}{N}\sum_{k=1}^{N} a_k^2 = SNR_{SIMO} \times Z, \quad (11)$$

where $SNR_{SIMO} = N\gamma$ is the average equivalent signal-to-noise-ratio of the overall SIMO system, which represents the power gain of using a higher number of receivers[5]. On the other hand, in (11), $Z = \frac{1}{N}\sum_{k=1}^{N} a_k^2$ is the diversity gain, which converges to 1 as the number of antennas increases (assuming each of the channel gains is normalized to have unit variance) and it hence helps overcome fading [9, P. 72]. In our simulations, we compare the EVM obtained in a SIMO channel to that of the SISO channel. Our goal is to study the diversity gain obtained by employing multiple receive antennas and not the power gain. Hence, we compare the SIMO channel to an equivalent SISO AWGN channel having a signal-to-noise-ratio of $SNR_{SISO} = SNR_{SIMO} = N\gamma$ in order to ensure the same average received power in both scenearios. Note that the BER or EVM performance of the SIMO system may be better than that of a SISO AWGN channel having an $SNR_{SISO} = \gamma$, but will always be worse than that of a SISO AWGN channel having an $SNR_{SISO} = SNR_{SIMO} = N\gamma$.

Now, employing the instantaneous SNR in (10) we obtain the instantaneous EVM to be $\text{EVM}(z) = \sqrt{\frac{1}{SNR_{SIMO} \times z}}$ for $L \to \infty$, where EVM(z) is the instantaneous EVM for the scenario of the diversity gain $Z = z$. The average EVM is formulated by employing the definition in [24] where, the average EVM is calculated by averaging over all possible values of z using the following expression:

$$\text{EVM} = \int_0^{\infty} \text{EVM}(z) f_Z(z) \mathrm{d}z, \quad (12)$$

[5]We employ the notation SNR_{SIMO} for distinguishing between the power gain and diversity gain obtained by employing multiple receive antennas.

where $f_Z(z)$ is the pdf of Z. Let us now derive the exact closed-form expressions for the EVM in a SIMO channel, while considering two fading scenarios, namely the η-μ and κ-μ shadowed fading channels.

A. η-μ Fading SIMO Channel

In order to derive the EVM for η-μ fading, we first have to derive the pdf of $Z = \sum_{k=1}^{N} X_k$, where we have $X_k = \frac{1}{N} a_k^2$. Thus, each X_k has the pdf given in (3) with $\bar{x}_k = E\{X_k\} = \frac{1}{N}$ and the distribution parameters of $\{\eta_k, \mu_k\}$. The moment generating function (MGF) for X_k has been derived in [26]. In [27], it has been shown that the MGF of X_k can be represented as the product of the MGFs of two gamma distributed RVs (RVs), where both these gamma RVs have the same shape parameter $\alpha_{2k-1} = \alpha_{2k} = \mu_k$, but different scale parameters of $\theta_{2k-1} = \frac{\bar{x}_k}{2\mu_k(h_k+H_k)}$ and $\theta_{2k} = \frac{\bar{x}_k}{2\mu_k(h_k-H_k)}$. Using this relationship, as well as the studies in [27] and [28], we can state that $X_k = P_k + Q_k$, such that $P_k \sim \mathcal{G}(\alpha_{2k-1}, \theta_{2k-1})$, and $Q_k \sim \mathcal{G}(\alpha_{2k}, \theta_{2k})$. Note that $\mathcal{G}(\alpha_{2k}, \theta_{2k})$ denote the gamma distribution with shape parameter α_{2k} and scale parameter θ_{2k}. Thus, the sum of N η-μ RVs may be alternatively expressed as the sum of $L = 2N$ Gamma RVs, where the pdf of the sum of L Gamma RVs has been derived in [29]. Now, as stated earlier, the pdf of $Z = \sum_{k=1}^{N} X_k$ has been derived to be the following using the pdf of the sum of $2N$ Gamma RVs [29]:

$$f_{Z,\eta-\mu}(z) = \frac{z^{\sum_{i=1}^{2N}\alpha_i - 1}}{\prod_{i=1}^{2N}(\theta_i)^{\alpha_i}\,\Gamma\left(\sum_{i=1}^{2N}\alpha_i\right)} \Phi_2^{(2N)}\left(\alpha_1, \cdots, \alpha_{2N}; \sum_{i=1}^{2N}\alpha_i; \frac{-z}{\theta_1}, \cdots, \frac{-z}{\theta_{2N}}\right), \quad (13)$$

where $\Phi_2^{(N)}(.)$ is the confluent Lauricella function [30]. We can now substitute this $f_{Z,\eta-\mu}(z)$ into (12) for formulating the average EVM.

1) EVM of η-μ SIMO Channel With Independent and Nonidentically Distributed Branches:

Lemma 1: The EVM expression of the η-μ fading SIMO channel having independent and non-identically distributed (i.n.i.d) branches is given by

$$EVM_{\eta-\mu,i.n.i.d} = \frac{\sqrt{N\mu_1(1+\eta_1^{-1})}}{\sqrt{SNR_{SIMO}}} \frac{\Gamma(2\sum_{i=1}^{N}\mu_i - 0.5)}{\Gamma(2\sum_{i=1}^{N}\mu_i)} \times F_D^{(2N-1)}\Bigg[0.5, \mu_1, \mu_2, \mu_2, \cdots, \mu_N, \mu_N; 2\sum_{i=1}^{N}\mu_i; 1 - \frac{1}{\eta_1}, 1 - \frac{\mu_1(1+\eta_1^{-1})}{\mu_2(1+\eta_2^{-1})}, 1 - \frac{\mu_1(1+\eta_1^{-1})}{\mu_2(1+\eta_2)} \cdots 1 - \frac{\mu_1(1+\eta_1^{-1})}{\mu_N(1+\eta_N^{-1})}, 1 - \frac{\mu_1(1+\eta_1^{-1})}{\mu_N(1+\eta_N)}\Bigg] \quad (14)$$

for $2\sum_{i=1}^{N}\mu_i > 0.5$.

Proof: See Appendix I for the proof. ■

The expression of the EVM for the i.n.i.d case is given in terms of Lauricella's function of the fourth kind $F_D^{(N)}[.]$ [30]. The function $F_D^{(N)}[a, b_1, \cdots, b_N; c; x_1, \cdots, x_N]$ can be evaluated using the following single integral expression:

$$\frac{\Gamma(c)}{\Gamma(a)\Gamma(c-a)} \int_0^1 t^{a-1}(1-t)^{c-a-1} \prod_{i=1}^{N} (1-x_i t)^{-b_i} \mathrm{d}t, \quad \text{where } \mathrm{Real}(c) > \mathrm{Real}(a) > 0, \tag{15}$$

where Real(.) returns the real part of the argument. Note that the condition $\mathrm{Real}(c) > \mathrm{Real}(a) > 0$ is satisfied by Lauricella's function of the fourth kind $F_D^{(N)}[.]$, which appeared in (14).

Special Case 1: Now, we simplify the expression in (14) for the case of independent and identically distributed (i.i.d) fading SIMO channels. Substituting both $\eta_i = \eta$ and $\mu_i = \mu \ \forall i$ into (14) and then using the following identity:

$$F_D^{(N)}[a, b_1, \cdots b_n; c, x, \cdots, x] = 2F_1[a, b_1 + \cdots + b_N; c; x], \tag{16}$$

where ${}_2F_1[.]$ is the Gauss hypergeometric function [30], we obtain,

$$\mathrm{EVM}_{\eta-\mu,i.i.d} = \frac{\sqrt{N\mu(1+\eta^{-1})}}{\sqrt{SNR_{SIMO}}} \frac{\Gamma(2N\mu - 0.5)}{\Gamma(2N\mu)} {}_2F_1[0.5, N\mu; 2N\mu; 1 - \frac{1}{\eta}] \text{ for } 2N\mu > 0.5. \tag{17}$$

In the following, we show that the expression shown in (17) converges to the EVM expression of AWGN channel. Note that when fading parameters $\eta = 1$ and μ tends to infinity, the η-μ channel should converge to an AWGN channel. By substituting $\eta = 1$ and $\mu \to \infty$ in (17), it can be simplified to

$$\mathrm{EVM}_{AWGN} = \lim_{\mu \to \infty} \frac{\sqrt{2N\mu}}{\sqrt{SNR_{SIMO}}} \frac{\Gamma(2N\mu - 0.5)}{\Gamma(2N\mu)} = \frac{1}{\sqrt{SNR_{SIMO}}}. \tag{18}$$

This simplification follows from the fact that ${}_2F_1[0.5, N\mu; 2N\mu; 0] = 1$. We now provide the upper bound of the EVM expression given in (17) so that the impact of fading parameter η can be shown. Using the transformation ${}_2F_1[a, b; c; z] = (1-z)^{c-a-b}_2 F_1[c-a, c-b; c; z]$, we obtain:

$$\mathrm{EVM}_{\eta-\mu,i.i.d} = \frac{\sqrt{N\mu(1+\eta^{-1})}}{\sqrt{SNR_{SIMO}}} \frac{\Gamma(2N\mu - 0.5)}{\Gamma(2N\mu)} {}_2F_1[2N\mu - 0.5, N\mu; 2N\mu; 1 - \frac{1}{\eta}] \left(\frac{1}{\eta}\right)^{\mu - 0.5}, \tag{19}$$

and using the bound ${}_2F_1[2N\mu - 0.5, N\mu; 2N\mu; 1 - \frac{1}{\eta}] <_2 F_1[2N\mu, N\mu; 2N\mu; 1 - \frac{1}{\eta}] \left(\frac{1}{\eta}\right)^{-\mu}$, the expression given in (19) can be upper bounded as:

$$\mathrm{EVM}_{\eta-\mu,i.i.d} < \frac{\sqrt{N\mu(1+\eta^{-1})}}{\sqrt{SNR_{SIMO}}} \frac{\Gamma(2N\mu - 0.5)}{\Gamma(2N\mu)} \left(\frac{1}{\eta}\right)^{-0.5} = \frac{\sqrt{N\mu(1+\eta)}}{\sqrt{SNR_{SIMO}}} \frac{\Gamma(2N\mu - 0.5)}{\Gamma(2N\mu)}. \tag{20}$$

Hence, it is apparent from (20) that as η increases, the EVM increases. Recall that η is the scattered-wave power ratio between the in-phase and quadrature components of each cluster of multipath and hence the EVM will be minimum when the power of the in-phase and the quadrature components is equal.

Special Case 2: The Nakagami-m fading is a special case of the η-μ fading associated with $\eta = 1$ and $2\mu = m'$. Note that m' is the shape parameter of the Nakagami-m fading. Substituting $\eta = 1$ and $2\mu = m$ in (14) and (17), we obtain the following expressions for the i.n.i.d and i.i.d scenarios, respectively:

$$\mathrm{EVM}_{n,i.n.i.d} = \frac{\sqrt{Nm'_1}}{\sqrt{SNR_{SIMO}}} \frac{\Gamma(\sum_{i=1}^{N} m'_i - 0.5)}{\Gamma(\sum_{i=1}^{N} m'_i)} \times F_D^{(N-1)}\left[0.5, m'_2, \cdots, m'_N; \sum_{i=1}^{N} m'_i; 1 - \frac{m'_1}{m'_2}, \cdots, 1 - \frac{m'_1}{m'_N}\right] \text{ for } \sum_{i=1}^{N} m'_i > 0.5 \text{ and} \tag{21}$$

$$\mathrm{EVM}_{n,i.i.d} = \frac{\sqrt{Nm'}}{\sqrt{SNR_{SIMO}}} \frac{\Gamma(Nm' - 0.5)}{\Gamma(Nm')} \text{ for } Nm' > 0.5. \tag{22}$$

Using the following identity from [31]:

$$\frac{\Gamma(n+a)}{\Gamma(n+b)} = n^{a-b}\left(1 + \frac{(a-b)(a+b-1)}{2n} + O(|n|^{-2})\right) \text{ for large } n, \tag{23}$$

the EVM of the i.i.d Nakagami-m scenario can be further simplified to

$$\mathrm{EVM}_{n,i.i.d} = \frac{1}{\sqrt{SNR_{SIMO}}}\left(1 + \frac{0.75}{2Nm'} + O(|Nm'|^{-2})\right) \text{ for large } Nm'. \tag{24}$$

Note that the first term in (24) represents the EVM of an AWGN channel, while the remaining terms in (24) represent the contribution of the fading. We know that as the parameter m decreases, the impact of fading becomes more severe, which is confirmed by (24). A second point that may be noted from (24) is that the EVM approaches that of an AWGN channel, when the number of receive antennas tends to infinity and/or when the fading parameter tends to infinity.

2) EVM of η-μ SIMO Channel With Correlated and Identically Distributed Branches:

Lemma 2: The EVM expression of a correlated η-μ SIMO channel associated with an MRC-based receiver is given by:

$$\mathrm{EVM}_{\eta-\mu,corr} = \frac{1}{\sqrt{\hat{\theta}_1 SNR_{SIMO}}} \frac{\Gamma(2N\mu_c - 0.5)}{\Gamma(2N\mu_c)} \times F_D^{(2N-1)}\left(0.5, \mu_c, \cdots, \mu_c; 2N\mu_c; 1-\frac{\hat{\theta}_2}{\hat{\theta}_1}, \cdots 1-\frac{\hat{\theta}_{2N}}{\hat{\theta}_1}\right) \quad for\ 2N\mu_c > 0.5. \tag{25}$$

Proof: See Appendix II for the proof. ■

B. κ-μ Shadowed Fading SIMO Channel

In order to derive the EVM of a κ-μ shadowed faded channel, we first have to derive the pdf of $Z = \sum_{k=1}^{N} X_k$, where $X_k = \frac{1}{N} a_k^2$. Thus, each X_k has the pdf given in (5) with $\bar{x}_k = \frac{1}{N}$ and distribution parameters of $\{\kappa_k, \mu_k, m_k\}$. The pdf of Z has been shown in [11] to be as follows:

$$f_{Z,\kappa-\mu sh}(z) = \prod_{i=1}^{N} \frac{\mu_i^{\mu_i} m_i^{m_i} (1+\kappa_i)^{\mu_i} z^{\sum_{i=1}^{N}\mu_i - 1}}{\Gamma(\sum_{i=1}^{N}\mu_i)(\mu_i\kappa_i + m_i)^{m_i}\bar{x}_i^{\mu_i}} \cdot \Phi_2^{(N)}\left(\mu_1 - m_1, \cdots \mu_N - m_N, m_1 \cdots m_n; \sum_{i=1}^{N}\mu_i; -\frac{\mu_1(1+\kappa_1)z}{\bar{x}_1}, \cdots, -\frac{\mu_N(1+\kappa_N)z}{\bar{x}_N}, -\frac{\mu_1 m_1(1+\kappa_1)z}{(\mu_1\kappa_1 + m_1)\bar{x}_1} \cdots -\frac{\mu_N m_N(1+\kappa_N)z}{(\mu_N\kappa_N + m_N)\bar{x}_N}\right). \tag{26}$$

We can now substitute $f_{Z,\kappa-\mu sh}(z)$ in (12) to obtain the average EVM.

1) EVM of κ-μ Shadowed Fading SIMO Channel With i.n.i.d Branches:

Lemma 3: The EVM expression of κ-μ shadowed fading SIMO channel having i.n.i.d branches is given by

$$EVM_{\kappa-\mu sh,i.n.i.d} = \frac{\sqrt{N\mu_1(1+\kappa_1)}}{\sqrt{SNR_{SIMO}}} \frac{\Gamma\left(\sum_{i=1}^{N}\mu_i - 0.5\right)}{\Gamma\left(\sum_{i=1}^{N}\mu_i\right)} F_D^{(2N-1)}\Big(0.5, \mu_2 - m_2, \cdots, \mu_2 - m_2, m_1, \cdots m_N; \sum_{i=1}^{N}\mu_i; 1-\frac{\mu_1(1+\kappa_1)}{\mu_2(1+\kappa_2)}, \cdots, 1-\frac{\mu_1(1+\kappa_1)}{\mu_N(1+\kappa_N)}, 1-\frac{(\mu_1\kappa_1+m_1)}{m_1} \cdots 1-\frac{(\mu_N\kappa_N+m_N)\mu_1(1+\kappa_1)}{m_N\mu_N(1+\kappa_N)}\Big), \quad for \sum_{i=1}^{N}\mu_i > 0.5. \tag{27}$$

Proof: See Appendix III for the proof. ■

Special Case 1: Now, we simplify the expression in (27) for the i.i.d scenario, where we set $\mu_i = \mu$ and $\kappa_i = \kappa\ \forall i$ to obtain:

$$\mathrm{EVM}_{\kappa-\mu sh,i.i.d} = \frac{\sqrt{N\mu(1+\kappa)}}{\sqrt{SNR_{SIMO}}} \frac{\Gamma(N\mu - 0.5)}{\Gamma(N\mu)} {}_2F_1[0.5, Nm; , N\mu; -\frac{\mu\kappa}{m}] \text{ for } N\mu > 0.5. \tag{28}$$

In the following, we will show that the above expression converges to the EVM expression of AWGN channel. Note that when fading parameters $\kappa = 0$ and μ tends to infinity, the κ-μ channel should converge to an AWGN channel. By putting $\kappa = 0$ and $\mu \to \infty$ the above expression can be simplified to

$$\mathrm{EVM}_{AWGN} = \lim_{\mu\to\infty} \frac{\sqrt{N\mu}}{\sqrt{SNR_{SIMO}}} \frac{\Gamma(N\mu - 0.5)}{\Gamma(N\mu)} = \frac{1}{\sqrt{SNR_{SIMO}}}. \tag{29}$$

The above simplification follows from the fact that ${}_2F_1[0.5, N\mu; 2N\mu; 0] = 1$. Note that the EVM expression for an κ-μ shadowed channel converges to the expression of AWGN channel when fading parameter $\kappa = 0$ and μ tends to infinity, as expected.

Special Case 2: We now derive the closed-form expression of EVM for the κ-μ fading SIMO channel having i.i.d branches. Note that the κ-μ fading is a special case of the κ-μ shadowed fading with $m \to \infty$. Using the following identity [32]:

$$\lim_{b\to\infty} {}_2F_1\left[a, b, c, \frac{z}{b}\right] = {}_1F_1[a, c, z], \tag{30}$$

the ${}_2F_1[.]$ given in (28) can be simplified for $m \to \infty$ as follows:

$${}_2F_1[0.5, Nm; , N\mu; , -\frac{\mu\kappa}{m}] = 1F_1[0.5; N\mu; -N\mu\kappa], \tag{31}$$

where ${}_1F_1[.]$ is the Kummer hypergeometric function [30]. Therefore, the EVM expression of the κ-μ fading SIMO channel having i.i.d branches is given by

$$\mathrm{EVM}_{\kappa-\mu,i.i.d} = \frac{\sqrt{N\mu(1+\kappa)}}{\sqrt{SNR_{SIMO}}} \frac{\Gamma(N\mu - 0.5)}{\Gamma(N\mu)} {}_1F_1(0.5, N\mu, -N\mu\kappa) \text{ for } N\mu > 0.5. \tag{32}$$

The EVM expression of the κ-μ fading SISO channel is given by

$$\mathrm{EVM}_{\kappa-\mu} = \frac{\sqrt{\mu(1+\kappa)}}{\sqrt{SNR}} \frac{\Gamma(\mu - 0.5)}{\Gamma(\mu)} 1F_1(0.5, \mu, -\mu\kappa) \quad \text{for } \mu > 0.5. \tag{33}$$

Additional validation of Equation (33): In the following, we derive the EVM expression of the κ-μ fading SISO channel using the negative moment given in [10] in order to further validate our derivations[6]. The EVM for κ-μ channel is

[6]Note that the negative moment of sum of generalized fading distribution is not available and hence we cannot derive the EVM expression for SIMO channel.

given by

$$\text{EVM}_{\kappa-\mu} = \int_{a=0}^{\infty} \sqrt{\frac{1}{a^2\text{SNR}}}\, f_{\kappa-\mu}(a)\text{d}a$$

where $f_{\kappa-\mu}(a)$ is the κ-μ envelope probability density function. It is apparent from the above expression that the $\text{EVM}_{\kappa-\mu}$ is the negative moment of the κ-μ fading distribution. Using the moment expression given in [10], the $\text{EVM}_{\kappa-\mu}$ can be obtained as

$$\text{EVM}_{\kappa-\mu} = \frac{\sqrt{\mu(1+\kappa)}}{\sqrt{SNR}} \frac{\Gamma(\mu-0.5)\exp(-\kappa\mu)}{\Gamma(\mu)} {}_1F_1(\mu-0.5, \mu, \mu\kappa) \text{ for } \mu > 0.5. \quad (34)$$

Then, using the transformation $e_1^{-z}F_1(b-a, b, z) = 1F_1(a, b, -z)$, we can simplify the above expression to

$$\text{EVM}_{\kappa-\mu} = \frac{\sqrt{\mu(1+\kappa)}}{\sqrt{SNR}} \frac{\Gamma(\mu-0.5)}{\Gamma(\mu)} 1F_1(0.5, \mu, -\mu\kappa). \quad (35)$$

Therefore, we have shown that the expressions given in (35) and (33) are same. Note that the functional form of the pdf of the sum of correlated κ-μ shadowed random variables is similar to that of the sum of correlated η-μ random variables. Hence, the EVM expression for a correlated κ-μ shadowed SIMO channel can be derived in a similar manner to that of the η-μ SIMO channel. Furthermore, κ-μ fading is a special case of κ-μ shadowed fading and hence the EVM can be obtained numerically by employing a very high value of m in the EVM expression for a κ-μ shadowed fading channel.

IV. Simulation Results

In order to validate the EVM expressions derived for η-μ and κ-μ shadowed fading channels associated with the arbitary parameters, we simulated a BPSK modulation-based system communicating over these channels. We implemented a simulation-based solution of (12) using 1 transmit and N receive antennas. The simulations employed the Monte Carlo approach, which relies on transmitting a large number of bits over the wireless channel and computing the average EVM. The simulations were carried out in Matlab.

Fig. 2 shows the EVM variation with respect to SNR_{SIMO} for the case of SIMO channels having independent and non-identically distributed branches, where it can be seen that the simulation results closely match the theoretical values.

Fig. 3 depicts the variation of EVM with respect to SNR_{SIMO} for η-μ fading. Here, we have considered $N = 3$ and $\eta \geq 1$, since η is symmetrical about 1. Firstly, it may be seen that the analytical results match with the simulation results for the entire range of SNR_{SIMO}. Secondly, it may be observed that as η increases, the EVM also increases for a fixed value of μ. Recall that η is the power ratio of the in-phase and quadrature-phase components of the fading signal in each multipath cluster. Hence, as the power ratio of the in-phase and quadrature-phase components increases, the EVM increases. In other words, the EVM would be minimum, when the power of the in-phase and quadrature-phase components of the fading signal in each multipath cluster is equal. Thirdly, as the shape parameter μ increases, the EVM decreases and it approaches the EVM of an AWGN channel.

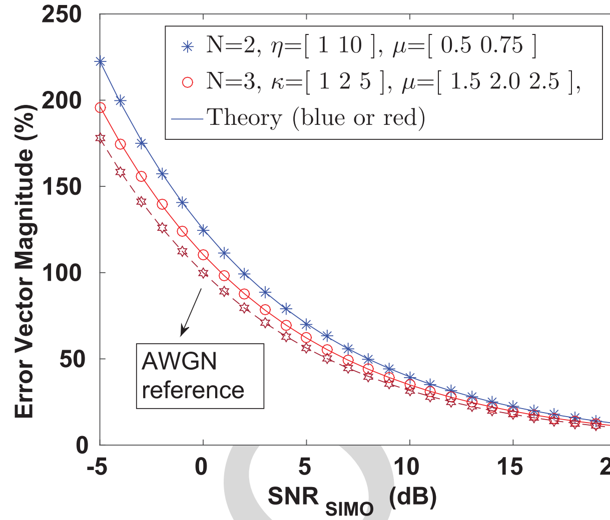

Fig. 2. The EVM for η-μ and κ-μ shadowed i.n.i.d SIMO channels.

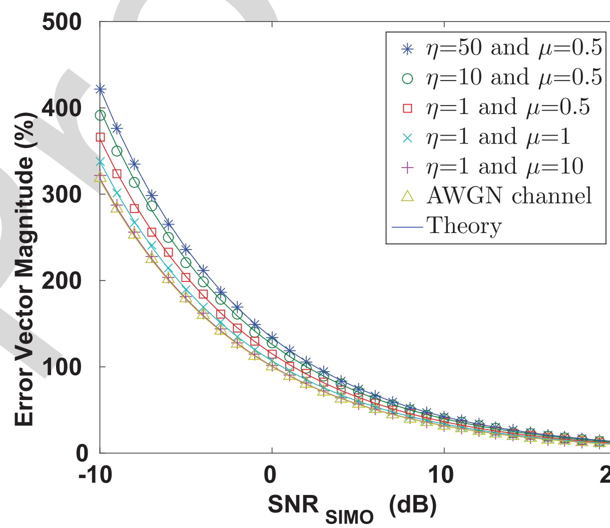

Fig. 3. The EVM for different values of η and μ, when $N = 3$ and the channels are i.i.d.

Fig. 4 shows the variation of EVM with respect to SNR_{SIMO} for different values of N. Firstly, observe that the simulation results closely match the analytical results. Secondly, as the number of antennas increases, the EVM decreases and it approaches the EVM of an AWGN channel. Interestingly, it may be seen that the EVM decreases significantly as the number of antennas increases from 1 to 2. However, the EVM reduction becomes less significant, as the number of antennas increases from $N = 2$ to 3 and so on.

Fig. 5 shows the variation of EVM as a function of SNR_{SIMO} for different values of correlation coefficients. The correlation between the SIMO branches is defined by the correlation matrix in (6) in conjunction with $\rho_{pq} = \rho^{|p-q|}$, where

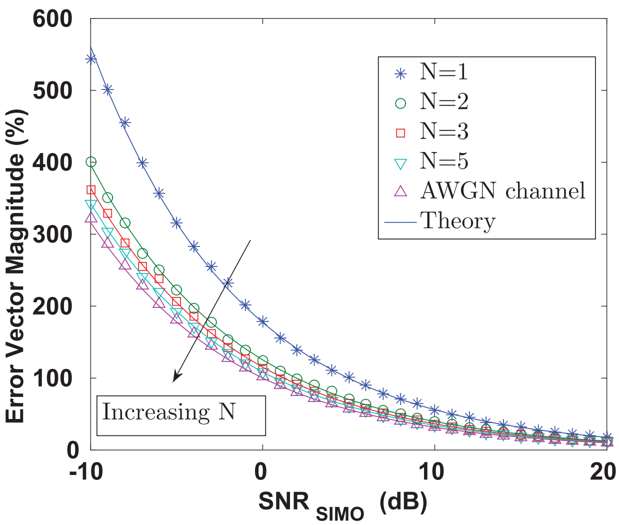

Fig. 4. The EVM for different values of N, when $\eta = 1$ and $\mu = 0.5$ and the channels are i.i.d.

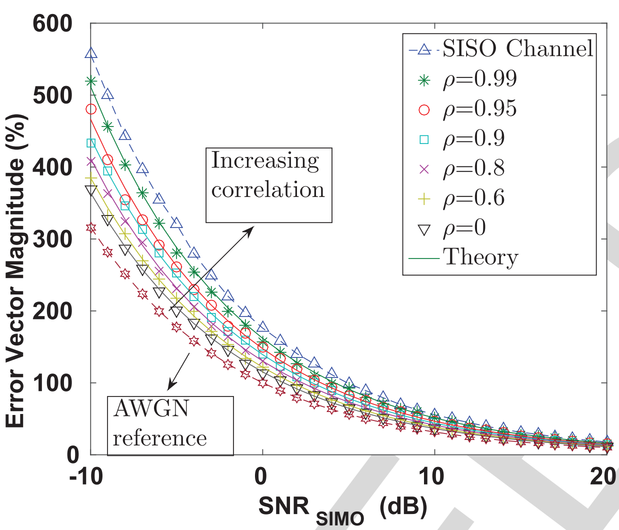

Fig. 5. The EVM for different values of correlation, when $N = 3$, while $\eta = 1$ and $\mu = 0.5$ for all the channels.

we have $p, q = 1, \cdots, N$. Firstly, it may be seen that the simulation results closely match the analytical results for all values of the correlation coefficients. Secondly, it is observed that the EVM increases, as the correlation among the branches increases and it approaches the EVM of a SISO channel. Furthermore, the rate at which the EVM increases is higher, when the correlation coefficients are high.

Fig. 6 shows the variation of EVM versus the $N \times m$ product for the special case of Nakagami channels. It may be seen that the EVM decreases, as either N or m increases. Interestingly, the rate at which the EVM decreases is higher, when the number of antennas and the Nakagami-m fading parameter are small. This phenomenon may also be observed from (24), where the EVM of the Nakagami-m fading is shown to be a function of $1/(N \times m)$.

Fig. 7 shows the EVM variation versus SNR_{SIMO} for κ-μ fading. Again, the simulation results closely match the analytical results. It may be seen that as κ increases, the EVM

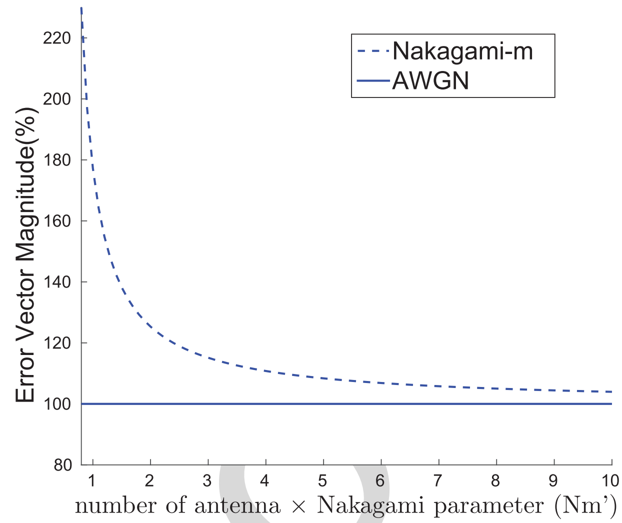

Fig. 6. Variation in EVM with respect to $N \times m'$ for a Nakagami SIMO channel which are i.i.d.

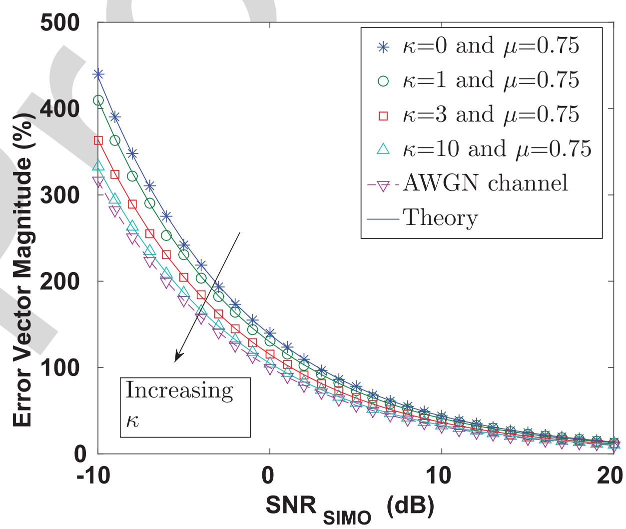

Fig. 7. The EVM for different combinations of κ and μ, when $N = 2$ and the channels are i.i.d.

decreases and it approaches the EVM of an AWGN channel. Recall that κ represents the ratio of the total power of the dominant components to that of the scattered waves. Hence, as the ratio of the total power of the dominant components to that of the scattered waves increases, the EVM decreases, as expected.

V. Conclusions

We have derived exact closed-form expressions for the data-aided EVM in η-μ and κ-μ shadow faded SIMO channels having independent and non-identically distributed branches. The EVM expression is also derived for the scenario of correlated SIMO branches. Furthermore, the expressions derived may be readily simplified for various special cases, such as independent and identically distributed fading, the Rayleigh, the Nakagami-m and finally the κ-μ fading. Subsequently, we performed a simulation based study of this system in order to validate the analytical results. Finally, a parametric study of the

EVM performance of the wireless communication system considered showed that as the Nakagami fading parameter m and/or the number of antennas N increases, the EVM decreases and the rate at which the EVM decreases is higher, when the fading parameter and/or the number of antennas is small.

ACKNOWLEDGMENT

We are grateful to Dr. R. A. Shafik for his valuable inputs.

APPENDIX A

The EVM for a AWGN SISO channel is given by (10) [23], [24]. Thus, the instantaneous EVM, namely $EVM(z)$, is computed using (10) but with the replacement of SNR_{SISO} with the instantaneous signal-to-noise ratio, where $zSNR_{SIMO}$ is the instantaneous signal-to-noise ratio as per (11). Thus, the EVM of a η-μ fading channel is defined as follows [24]:

$$\mathrm{EVM}_{\eta-\mu,i.n.i.d} = \int_0^\infty \mathrm{EVM}(z)\, f_{Z,\eta-\mu}(z)\mathrm{d}z, \tag{36}$$

which simply weights the AWGN channel's EVM by the specific probability of occurance of each particular instantaneous SNR given by its distribution and then averages it by integrating it across the entire instantaneous SNR range. Now substituting (13) in (36), we get:

$$\begin{aligned}\mathrm{EVM}_{\eta-\mu,i.n.i.d} &= \int_0^\infty \sqrt{\frac{1}{zSNR_{SIMO}}}\frac{z^{\sum_{i=1}^{2N}\alpha_i-1}}{\prod_{i=1}^{2N}(\theta_i)^{\alpha_i}\Gamma\left(\sum_{i=1}^{2N}\alpha_i\right)}\cdot\\ &\quad \Phi_2^{(2N)}\left(\alpha_1,\cdots,\alpha_{2N};\sum_{i=1}^{2N}\alpha_i;\frac{-z}{\theta_1},\cdots,\frac{-z}{\theta_{2N}}\right)\mathrm{d}z\\ &= \int_0^\infty \sqrt{\frac{1}{SNR_{SIMO}}}\frac{z^{\sum_{i=1}^{2N}\alpha_i-1.5}}{\prod_{i=1}^{2N}(\theta_i)^{\alpha_i}\Gamma\left(\sum_{i=1}^{2N}\alpha_i\right)}\\ &\quad \Phi_2^{(2N)}\left(\alpha_1,\cdots,\alpha_{2N};\sum_{i=1}^{2N}\alpha_i;\frac{-z}{\theta_1},\cdots,\frac{-z}{\theta_{2N}}\right)\mathrm{d}z.\end{aligned} \tag{37}$$

Using the transformation [30, P. 177]:

$$\begin{aligned}&e^{-x_i}\Phi_2^{(n)}(b_1,\cdots,b_n;c;x_1,\cdots,x_n)\\ &\quad=\Phi_2^{(n)}(b_1,\cdot,b_{i-1},c-b_1-\cdot-b_n,b_{i+1},\cdot,b_n;c;\\ &\quad x_1-x_i,\cdots x_{i-1}-x_i,-x_i,x_{i+1}-x_i,\cdot,x_n-x_i),\end{aligned} \tag{38}$$

the $\mathrm{EVM}_{\eta-\mu,i.n.i.d}$ can be rewritten as:

$$\begin{aligned}\mathrm{EVM}_{\eta-\mu,i.n.i.d} &= K_1\int_0^\infty z^{\sum_{i=1}^{2N}\alpha_i-1.5}e^{-\frac{z}{\theta_1}}\\ &\quad\times\Phi_2^{(2N)}\left(0,\alpha_2,\cdots,\alpha_{2N};\sum_{i=1}^{2N}\alpha_i;\frac{z}{\theta_1},\left(\frac{1}{\theta_1}-\frac{1}{\theta_2}\right)z,\right.\\ &\quad\left.\cdots\left(\frac{1}{\theta_1}-\frac{1}{\theta_N}\right)z\right)\mathrm{d}z,\end{aligned} \tag{39}$$

where we have $K_1=\sqrt{\frac{1}{SNR_{SIMO}}}\frac{1}{\prod_{i=1}^{2N}(\theta_i)^{\alpha_i}\Gamma\left(\sum_{i=1}^{2N}\alpha_i\right)}$. Note that if one of the numerator parameters of the series expansion of $\Phi_2^{(N)}$ goes to zero, then $\Phi_2^{(N)}$ becomes $\Phi_2^{(N-1)}$ and hence the above $\Phi_2^{(2N)}$ will become $\Phi_2^{(2N-1)}$ with appropriate parameters. Using the transformation $\frac{z}{\theta_1}=t$ we obtain:

$$\begin{aligned}\mathrm{EVM}_{\eta-\mu,i.n.i.d} &= K_1\theta_1^{\sum_{i=1}^{2N}\mu_i-0.5}\int_0^\infty t^{\sum_{i=1}^{2N}\alpha_i-1.5}e^{-t}\\ &\quad\times\Phi_2^{(2N-1)}\left(\alpha_2,\cdots,\alpha_{2N};\sum_{i=1}^{2N}\alpha_i;\left(1-\frac{\theta_1}{\theta_2}\right)t,\right.\\ &\quad\left.\cdots\left(1-\frac{\theta_1}{\theta_N}\right)t\right)\mathrm{d}t.\end{aligned} \tag{40}$$

Using the following identity [30, P. 51]:

$$\begin{aligned}&F_D^{(n)}[a,b_1,\cdots,b_n,c,x_1,\cdots,x_n]\\ &=\frac{1}{\Gamma(a)}\int_{t=0}^\infty e^{-t}t^{a-1}\Phi_2^{(n)}[b_1,\cdots,b_n,c,x_1t,\cdots,x_nt]\mathrm{d}t,\end{aligned} \tag{41}$$

where $\mathrm{Real}(a)>0$, one obtains:

$$\begin{aligned}\mathrm{EVM}_{\eta-\mu,i.n.i.d} &= K_1\theta_1^{\sum_{i=1}^{2N}\alpha_i-0.5}\Gamma\left(\sum_{i=1}^{2N}\alpha_i-0.5\right)\\ &\quad\times F_D^{(2N-1)}\left(\sum_{i=1}^{2N}\alpha_i-0.5,\alpha_2,\cdots,\alpha_{2N};\sum_{i=1}^{2N}\alpha_i;\right.\\ &\quad\left.1-\frac{\theta_1}{\theta_2},\cdots,1-\frac{\theta_1}{\theta_N}\right)\end{aligned} \tag{42}$$

for $\sum_{i=1}^{2N}\alpha_i>0.5$. Here $F_D^{(N)}[a,b_1,\cdots,b_N;c;x_1,\cdots,x_N]$ is the Lauricella's function of the fourth kind. Again, using the following identity:

$$\begin{aligned}&F_D^{(n)}[a,b_1,\cdots,b_n,c,x_1,\cdots,x_n]=\prod_{i=1}^n(1-x_i)^{-b_i}\\ &F_D^{(n)}[a,b_1,\cdots,b_n,c,\frac{x_1}{x_1-1},\cdots,\frac{x_n}{x_n-1}],\end{aligned} \tag{43}$$

we arrive at:

$$\begin{aligned}\mathrm{EVM}_{\eta-\mu,i.n.i.d} &= K_1\theta_1^{\sum_{i=1}^{2N}\alpha_i-0.5}\Gamma\left(\sum_{i=1}^{2N}\alpha_i-0.5\right)\prod_{i=2}^{2N}\left(\frac{\theta_1}{\theta_i}\right)^{-\alpha_i}\\ &\times F_D^{(2N-1)}\left(0.5,\alpha_2,\cdots,\alpha_{2N};\sum_{i=1}^{2N}\alpha_i;1-\frac{\theta_2}{\theta_1},\cdots,1-\frac{\theta_{2N}}{\theta_1}\right).\end{aligned} \tag{44}$$

Substituting the value of K_1, the $\mathrm{EVM}_{\eta-\mu,i.n.i.d}$ expression can be simplified to

$$\mathrm{EVM}_{\eta-\mu,i.n.i.d} = \frac{1}{\sqrt{\theta_1 SNR_{SIMO}}} \frac{\Gamma(\sum_{i=1}^{2N} \alpha_i - 0.5)}{\Gamma(\sum_{i=1}^{2N} \alpha_i)} \times F_D^{(2N-1)}\left(0.5, \alpha_2, \cdots, \alpha_{2N}; \sum_{i=1}^{2N} \alpha_i; 1-\frac{\theta_2}{\theta_1}, \cdots, 1-\frac{\theta_{2N}}{\theta_1}\right). \tag{45}$$

Substituting the value of θ_i, α_i and $\bar{z} = 1/N$ into (45), we obtain the final expression of $\mathrm{EVM}_{\eta-\mu,i.n.i.d}$ given in (14).

Appendix B

The underlying philosophy in this derivation is similar to that of an $\eta - \mu$ SIMO channel with i.n.i.d branches. We now consider the scenario studies in this paper, where Z is the sum of N correlated and identically distributed η-μ RVs X_k having distribution parameters $\{\eta_k, \mu_c\}$. Note that all the X_ks have the same μ_c but different η_k. As discussed in the first paragraph of Section III-A, an η-μ random variable may be expressed as the sum of two independent Gamma distributed RVs. It has been discussed in [28] that each X_k may be expressed as

$$X_k = P_k + Q_k, \tag{46}$$

where $P_k \sim \mathcal{G}(\mu_c, \theta_{2k-1})$, and $Q_k \sim \mathcal{G}(\mu_c, \theta_{2k})$ with $\theta_{2k-1} = \frac{\bar{x}_k}{2\mu_c(h_k+H_k)}$ and $\theta_{2k} = \frac{\bar{x}_k}{2\mu_c(h_k-H_k)}$. Similar to Section III-A, $\bar{x}_k = 1/N$, while h_k and H_k are given by (4). Note that the correlation among the different X_ks results in a correlation among the different P_ks and among the Q_ks, but there is no correlation between the P_ks and Q_ks. If ρ_{ij}^{xx} is the correlation between $X_i = P_i + Q_i$ and $X_j = P_j + Q_j$, while ρ_{ij}^{pp} and ρ_{ij}^{qq} is the correlation between $\{P_i, P_j\}$ and $\{Q_i, Q_j\}$, respectively then we have (47), shown at the bottom of the page.

In our study Z is the sum of N correlated and identically distributed η-μ RVs X_k. Employing (46), we may state that Z is the sum of $2N$ correlated and non-identically distributed Gamma distributed RVs M_i, namely $\{M_1 = P_1, M_2 = Q_1, M_3 = P_2, M_4 = Q_2 \ldots, M_{2N-1} = P_N, M_{2N} = Q_N\}$. The pdf of the sum of N correlated η-μ math RVs is given by [16], [29], [33]

$$F_{Z,\eta-\mu,corr}(z) = \frac{z^{2N\mu_c-1}}{\det(\mathbf{A})^{\mu_c}\Gamma(2N\mu_c)} \times \Phi_2^{(2N)}\left(\mu_c, \cdots, \mu_c; 2N\mu_c; \frac{-z}{\hat{\theta}_1}, \cdots, \frac{-z}{\hat{\theta}_{2N}}\right), \tag{48}$$

where $\hat{\theta}_i$ is the eigen values of $\mathbf{A} = \mathbf{DC}$ with $\mathbf{D}$ being a diagonal matrix with entries θ_i and $\det(\mathbf{A}) = \prod_{i=1}^{N} \hat{\theta}_i$ is the determinant of the matrix $\mathbf{A}$. Here, $\mathbf{C}$ is the symmetric positive definite (s.p.d) matrix and is given in (49), shown at the bottom of the page. where ρ_{ij}^{mm} denotes the correlation coefficient between M_i and M_j, and is given by,

$$\rho_{ij}^{mm} = \rho_{ji}^{mm} = \frac{\mathrm{cov}(M_i, M_j)}{\sqrt{\mathrm{var}(M_i)\mathrm{var}(M_j)}}, 0 \le \rho_{ij} \le 1, \tag{50}$$

with $\mathrm{cov}(M_i, M_j)$ being the covariance between M_i and M_j. Note that the alternate zeros are a consequence of P_ks and Q_ks being independent.

Just as in (36), the EVM of a SIMO channel encountering correlated η-μ fading and employing MRC reception is defined as follows:

$$\mathrm{EVM}_{\eta-\mu,corr} = \int_0^\infty \mathrm{EVM}(z)\ f_{Z,\eta-\mu,corr}(z)\mathrm{d}z, \tag{51}$$

The functional form of the pdf of the sum of correlated gamma RVs is similar to that of the sum of i.n.i.d. $\eta - \mu$ RVs, as given in (13). Hence the EVM expression in (51) may be readily simplified to:

$$\mathrm{EVM}_{\eta-\mu,corr} = \frac{1}{\sqrt{\hat{\theta}_1 SNR_{SIMO}}} \frac{\Gamma(2N\mu_c - 0.5)}{\Gamma(2N\mu_c)} \times F_D^{(2N-1)}\left(0.5, \mu_c, \cdots, \mu_c; 2N\mu_c; \left(1-\frac{\hat{\theta}_2}{\hat{\theta}_1}\right), \cdots \left(1-\frac{\hat{\theta}_{2N}}{\hat{\theta}_1}\right)\right) \tag{52}$$

Note that $\hat{\theta}_i$ is the eigen values of $\mathbf{A} = \mathbf{DC}$ with $\mathbf{D}$ being a diagonal matrix with entries θ_i and $\mathbf{C}$ is the symmetric positive definite (s.p.d) covariance matrix defined in (49).

$$\rho_{ij}^{xx} = \frac{\rho_{ij}^{pp}\sqrt{\mathrm{var}(P_i)\mathrm{var}(P_j)} + \rho_{ij}^{qq}\sqrt{\mathrm{var}(Q_i)\mathrm{var}(Q_j)}}{\sqrt{\mathrm{var}(P_i)\mathrm{var}(P_j) + \mathrm{var}(Q_i)\mathrm{var}(Q_j) + \mathrm{var}(P_i)\mathrm{var}(Q_j) + \mathrm{var}(P_j)\mathrm{var}(Q_i)}} \tag{47}$$

$$\mathbf{C} = \begin{bmatrix} 1 & 0 & \sqrt{\rho_{12}^{pp}} & 0 & \sqrt{\rho_{13}^{pp}} & 0 & \ldots & \sqrt{\rho_{1N}^{pp}} & 0 \\ 0 & 1 & 0 & \sqrt{\rho_{12}^{qq}} & 0 & \sqrt{\rho_{13}^{qq}} & \ldots & 0 & \sqrt{\rho_{1N}^{qq}} \\ \sqrt{\rho_{21}^{pp}} & 0 & 1 & 0 & \sqrt{\rho_{23}^{pp}} & 0 & \ldots & \sqrt{\rho_{2N}^{pp}} & 0 \\ \vdots & \vdots & \vdots & \vdots & \vdots & \vdots & \vdots & \vdots & \vdots \\ 0 & \sqrt{\rho_{N1}^{qq}} & 0 & \sqrt{\rho_{N2}^{qq}} & 0 & \sqrt{\rho_{N3}^{qq}} & \ldots & 0 & 1 \end{bmatrix}. \tag{49}$$

Appendix C

The pdf $f_{Z,\kappa-\mu sh}(z)$ is presented in (26). Assuming that $\beta_i = \frac{\bar{x}_i}{\mu_i(1+\kappa_i)}$ and $\delta_i = \frac{(\mu_i\kappa_i+m_i)\bar{x}_i}{\mu_i(1+\kappa_i)m_i}$, we can rewrite the pdf $f_{Z,\kappa-\mu sh}(z)$ as

$$f_{Z,\kappa-\mu sh}(z) = \left(\prod_{i=1}^{N} \frac{1}{\beta_i^{\mu_i-m_i}\delta_i^{m_i}}\right) \frac{z^{\sum_{i=1}^{N}\mu_i - 1}}{\Gamma\left(\sum_{i=1}^{N}\mu_i\right)} \times \Phi_2^{(2N)}\left(\mu_1 - m_1, \cdots, \mu_N - m_N, m_1 \cdots, m_N; \sum_{i=1}^{N}\mu_i; -\frac{z}{\beta_1}, \cdots, -\frac{z}{\beta_N}, -\frac{z}{\delta_1}, \cdots, \frac{z}{\delta_N}\right). \quad (53)$$

The EVM of κ-μ shadow fading SIMO channel with i.n.i.d branches is defined as follows [24]:

$$\text{EVM}_{\kappa-\mu sh,i.n.i.d} = \int_0^{\infty} \text{EVM}(z)\ f_{Z,\kappa-\mu sh}(z)\text{d}z. \quad (54)$$

Note that the functional form of the pdf of the sum of κ-μ shadowed RVs is similar to that of the sum of η-μ RVs, as given in (13). Hence the EVM of the κ-μ shadowed fading SIMO channel with i.n.i.d branches may be expressed as follows:

$$\text{EVM}_{\kappa-\mu sh,i.n.i.d} = \frac{1}{\sqrt{\beta_1 SNR_{SIMO}}} \frac{\Gamma\left(\sum_{i=1}^{N}\mu_i - 0.5\right)}{\Gamma\left(\sum_{i=1}^{N}\mu_i\right)} \times F_D^{(2N-1)}\left(0.5, \mu_2 - m_2, \cdots, \mu_2 - m_2, m_1, \cdots m_N; \sum_{i=1}^{N}\mu_i; 1 - \frac{\beta_2}{\beta_1}, \cdots, 1 - \frac{\beta_N}{\beta_1}, 1 - \frac{\delta_1}{\beta_1} \cdots 1 - \frac{\delta_N}{\beta_1}\right). \quad (55)$$

Substituting the value of β_i and δ_i and $\bar{x}_i = 1/N\ \forall i$ into (55), we obtain the final expression of $\text{EVM}_{\kappa-\mu sh,i.n.i.d}$, which is given in (27).

References

[1] J. Zhang, Z. Tan, H. Wang, Q. Huang, and L. Hanzo, "The effective throughput of MISO systems over κ-μ fading channels," *IEEE Trans. Veh. Technol.*, vol. 63, no. 2, pp. 943–947, Feb. 2014.

[2] V. Aalo, T. Piboongungon, and G. Efthymoglou, "Another look at the performance of MRC schemes in Nakagami-M fading channels with arbitrary parameters," *IEEE Trans. Commun.*, vol. 53, no. 12, pp. 2002–2005, Dec. 2005.

[3] D. Chen, L.-L. Yang, and L. Hanzo, "Multi-hop diversity aided multi-hop communications: A cumulative distribution function aware approach," *IEEE Trans. Commun.*, vol. 61, no. 11, pp. 4486–4499, Nov. 2013.

[4] L. Hanzo, S. X. Ng, T. Keller, and W. Webb, *Quadrature Amplitude Modulation*, 2nd ed. Hoboken, NJ, USA: Wiley, 2004.

[5] R. Vaughan, N. Scott, and D. White, "Eight hints for making and interpreting EVM measurements," Agilent Application Note, May 2005, pp. 1–12.

[6] R. Liu, Y. Li, H. Chen, and Z. Wang, "EVM estimation by analyzing transmitter imperfections mathematically and graphically," *Analog Integr. Circuits Signal Process.*, vol. 48, no. 3, pp. 257–262, Jan. 2014.

[7] A. Georgiadis, "Gain, phase imbalance, and phase noise effects on error vector magnitude," *IEEE Trans. Veh. Technol.*, vol. 53, no. 2, pp. 443–449, Mar. 2004.

[8] R. Shafik, S. Rahman, R. Islam, and N. Ashraf, "On the error vector magnitude as a performance metric and comparative analysis," in *Proc. Int. Conf. Emerg. Technol. (ICET)*, Nov 2006, pp. 27–31.

[9] D. Tse and P. Viswanath, *Fundamentals of Wireless Communication*. Cambridge, U.K.: Cambridge Univ. Press, 2005.

[10] M. D. Yacoub, "The κ-μ distribution and the η-μ distribution," *IEEE Antennas Propag. Mag.*, vol. 49, no. 1, pp. 68–81, Feb. 2007.

[11] J. Paris, "Statistical characterization of κ-μ shadowed fading," *IEEE Trans. Veh. Technol.*, vol. 63, no. 2, pp. 518–526, Feb. 2014.

[12] M. Arti, "Channel estimation and detection in hybrid satellite-terrestrial communication systems," *IEEE Trans. Veh. Technol.*, 2015, http://ieeexplore.ieee.org/xpl/login.jsp?tp=&arnumber=7156170, to be published.

[13] M. Arti and M. Bhatnagar, "Beamforming and combining in hybrid satellite-terrestrial cooperative systems," *IEEE Commun. Lett.*, vol. 18, no. 3, pp. 483–486, Mar. 2014.

[14] M. Arti and M. Bhatnagar, "Two-way mobile satellite relaying: A beamforming and combining based approach," *IEEE Commun. Lett.*, vol. 18, no. 7, pp. 1187–1190, Jul. 2014.

[15] M. Arti, "Imperfect CSI based maximal ratio combining in shadowed-rician fading land mobile satellite channels," in *Proc. 21st Nat. Conf. Commun. (NCC)*, Feb. 2015, pp. 1–6.

[16] M. Bhatnagar, "On the sum of correlated squared κ-μ shadowed random variables and its application to performance analysis of MRC," *IEEE Trans. Veh. Technol.*, vol. 64, no. 6, pp. 2678–2684, Jun. 2015.

[17] J. F. Paris, "Outage probability in η-μ/η-μ and κ-μ/η-μ interference-limited scenarios," *IEEE Trans. Commun.*, vol. 61, no. 1, pp. 335–343, Jan. 2013.

[18] D. da Costa and M. Yacoub, "Average channel capacity for generalized fading scenarios," *IEEE Commun. Lett.*, vol. 11, no. 12, pp. 949–951, Dec. 2007.

[19] S. Kumar, G. Chandrasekaran, and S. Kalyani, "Analysis of outage probability and capacity for κ-μ/η-μ faded channel," *IEEE Commun. Lett.*, vol. 19, no. 2, pp. 211–214, Feb. 2015.

[20] L. Hanzo, M. El-Hajjar, and O. Alamri, "Near-capacity wireless transceivers and cooperative communications in the MIMO era: Evolution of standards, waveform design, and future perspectives," *Proc. IEEE*, vol. 99, no. 8, pp. 1343–1385, Aug. 2011.

[21] M. Bhatnagar and M. Arti, "On the closed-form performance analysis of maximal ratio combining in shadowed-rician fading LMS channels," *IEEE Commun. Lett.*, vol. 18, no. 1, pp. 54–57, Jan. 2014.

[22] K. Gharaibeh, K. Gard, and M. Steer, "Accurate estimation of digital communication system metrics–SNR, EVM and ρ; in a nonlinear amplifier environment," in *Proc. ARFTG Microw. Meas. Conf.*, Dec. 2004, pp. 41–44.

[23] R. Shafik, S. Rahman, and R. Islam, "On the extended relationships among EVM, BER and SNR as performance metrics," in *Proc. Int. Conf. Elect. Comput. Eng. (ICECE)*, Dec. 2006, pp. 408–411.

[24] H. Mahmoud and H. Arslan, "Error vector magnitude to SNR conversion for nondata-aided receivers," *IEEE Trans. Wireless Commun.*, vol. 8, no. 5, pp. 2694–2704, May 2009.

[25] N. Ermolova and O. Tirkkonen, "Bivariate η-μ fading distribution with application to analysis of diversity systems," *IEEE Trans. Wireless Commun.*, vol. 10, no. 10, pp. 3158–3162, Oct. 2011.

[26] N. Y. Ermolova, "Moment generating functions of the generalized η-μ and κ-μ distributions and their applications to performance evaluations of communication systems," *IEEE Commun. Lett.*, vol. 12, no. 7, pp. 502–504, Jul. 2008.

[27] K. Peppas, F. Lazarakis, A. Alexandridis, and K. Dangakis, "Error performance of digital modulation schemes with MRC diversity reception over η-μ fading channels," *IEEE Trans. Wireless Commun.*, vol. 8, no. 10, pp. 4974–4980, Oct. 2009.

[28] N. Y. Ermolova and O. Tirkkonen, "Bivariate η-μ fading distribution with application to analysis of diversity systems," *IEEE Trans. Wireless Commun.*, vol. 10, no. 10, pp. 3158–3162, Oct. 2011.

[29] S. Kalyani and R. Karthik, "The asymptotic distribution of maxima of independent and identically distributed sums of correlated or non-identical gamma random variables and its applications," *IEEE Trans. Commun.*, vol. 60, no. 9, pp. 2747–2758, Sep. 2012.

[30] H. Exton, *Multiple Hypergeometric Functions and Applications*. New York, NY, USA: Halsted Press, Ellis Horwood, 1976.

[31] F. G. Tricomi and A. Erdlyi, "The asymptotic expansion of a ratio of gamma functions," *Pac. J. Math.*, vol. 1, no. 1, pp. 133–142, 1951.

[32] N. M. Temme, "Large parameter cases of the gauss hypergeometric function," *J. Comput. Appl. Math.*, vol. 153, no. 1, pp. 441–462, 2003.

[33] S. Kumar and S. Kalyani, "Coverage probability and rate for η-μ/κ-μ fading channels in interference-limited scenarios," *IEEE Trans. Wireless Commun.*, vol. 14, no. 11, pp. 6082–6096, Nov. 2015.

Varghese Antony Thomas received the B.E. (Hons.) degree in electrical and electronics engineering from Birla Institute of Technology and Science, Pilani (Goa Campus), India, in 2010, and the M.Sc. degree in wireless communications and the Ph.D. degree from the University of Southampton, Southampton, U.K., in 2011 and 2015, respectively. He is a Research Associate with Georgia Institute of Technology, Atlanta, GA, USA. As a Ph.D. student, he worked with the Wireless Communications Research Group of the University of Southampton. His research interests include optical communications, optical-wireless integration, backhaul for MIMO, and radio over fiber systems. He was the recipient of several academic awards including the Commonwealth Scholarship of the Government of U.K. and Mayflower Scholarship of University of Southampton.

Suman Kumar received the B.Tech degree in electronics and communication engineering from the Future Institute of Engineering and Management, Kolkata, India, in 2010. He is currently pursuing the Ph.D. degree at the Department of Electrical Engineering, IIT Madras, Chennai, India.

His research interests include performance analysis of mobile broadband wireless networks including frequency reuse, HetNets, hypergeometric functions, and generalized fading models. He was the recipient of the Best Paper Award at ICWMC-2012 held at Venice, Italy.

Sheetal Kalyani received the B.E. degree in electronics and communication engineering from Sardar Patel University, Gujarat, India, in 2002, and the Ph.D. degree in electrical engineering from the Indian Institute of Technology (IIT) Madras, Chennai, India, in 2008. She was a Senior Research Engineer with the Centre of Excellence in Wireless Technology, Chennai, India, from 2008 to 2012. She is is currently an Assistant Professor with the Department of Electrical Engineering, IIT Madras.

Her research interests include HetNets, extreme value theory, hypergeometric functions, generalized fading models, and statistical learning algorithms for prediction in wireless networks.

Mohammed El-Hajjar received the B.Eng. degree in electrical engineering from the American University of Beirut, Lebanon, in 2004, and the M.Sc. degree in radio frequency communication systems and the Ph.D. degree in wireless communications from the University of Southampton, Southampton, U.K., in 2005 and 2008, respectively. Following the Ph.D., he joined Imagination Technologies as a Design Engineer, where he worked on designing and developing Imagination's multistandard communications platform, which resulted in three patents. Since January 2012, he has been a Lecturer with the Southampton Wireless Research Group, School of Electronics and Computer Science, University of Southampton, Southampton, U.K. He has authored a Wiley-IEEE book and more than 60 journal and international conference papers. His research interests include the development of intelligent communications systems including energy-efficient transceiver design, multifunctional MIMO, millimetre wave communications, and radio over fibre systems.

K. Giridhar received the B.Sc. degree in applied sciences from PSG College of Technology, Coimbatore, India, the M.E. degree in electrical communications from Indian Institute of Science, Bangalore, India, and the Ph.D. degree in electrical engineering from the University of California, Santa Barbara, Santa Barbara, CA, USA. Between 1989 and 1990, he was a Member of Research Staff with CRL, Bharat Electronics, Bangalore, India, and between 1993 and 1994, was a Research Affiliate in electrical engineering with Stanford University, Stanford, CA, USA. Since 1994, he has been with the Department of Electrical Engineering, IIT Madras (IITM), Chennai, India.

He serves as a Consultant to many Telecom & VLSI companies in India, and was on a Sabbatical from 2004 to 2005 with Beceem Communications. He has been a Visiting Faculty at Sri Sathya Sai Institute of Higher Learning, Prasanthi Nilayam, Anantapur, India, and Stanford University. His research interests include adaptive signal processing and wireless communications systems, with an emphasis on various transceiver algorithms, custom air-interface design for strategic applications, and performance analysis of mobile broadband wireless networks including HetNets.

He is a Member of the Telecommunications and Computer Networks (TeNeT) Group at IITM. He actively collaborates with the Center of Excellence in Wireless Technology on MIMO-OFDM broadband access research, resulting in several contributions to IEEE 802.16m, and currently on proposals to LTE-A and 5G forums.

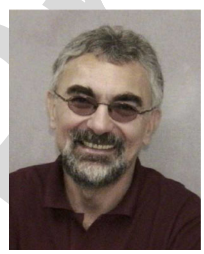

Lajos Hanzo (M'91–&SM'92–F'04) received the degree in electronics in 1976 and the doctorate degree in 1983. During his 40-year career in telecommunications, he has held various research and academic posts in Hungary, Germany, and the U.K. Since 1986, he has been with the School of Electronics and Computer Science, University of Southampton, U.K., where he holds the chair in telecommunications. He has successfully supervised about 100 Ph.D. students, co-authored 20 John Wiley/IEEE Press books on mobile radio communications totalling in excess of 10,000 pages, published over 1500 research entries at IEEE Xplore, acted both as the TPC and the General Chair of IEEE conferences, presented keynote lectures, and has been awarded a number of distinctions. Currently, he is directing a 60-strong academic research team, working on a range of research projects in the field of wireless multimedia communications sponsored by industry, the Engineering, and Physical Sciences Research Council (EPSRC), U.K., the European Research Council's Advanced Fellow Grant, and the Royal Society's Wolfson Research Merit Award. His research is funded by the European Research Council's Senior Research Fellow Grant. Lajos has over 23,000 citations. He is an enthusiastic supporter of industrial and academic liaison and offers a range of industrial courses. He is a Fellow of Royal Academy of Engineering, the Institution of Engineering and Technology, the EURASIP, and DSc. He is also a Governor of the IEEE VTS. From 2008 to 2012, he was the Editor-in-Chief of the IEEE Press and also a Chaired Professor at Tsinghua University, Beijing, China. In 2009, he was awarded an Honorary Doctorate by the Technical University of Budapest, while in 2015 by the University of Edinburgh.

Error Vector Magnitude Analysis of Fading SIMO Channels Relying on MRC Reception

Varghese Antony Thomas, Suman Kumar, Sheetal Kalyani, Mohammed El-Hajjar, K. Giridhar, and Lajos Hanzo, *Fellow, IEEE*

***Abstract*—We analytically characterize the data-aided error vector magnitude (EVM) performance of a single-input multiple-output (SIMO) communication system relying on maximal ratio combining (MRC) having either independent or correlated branches that are nonidentically distributed. In particular, exact closed form expressions are derived for the EVM in η-μ fading and κ-μ shadowed fading channels and these expressions are validated by simulations. The derived expressions are expressed in terms of Lauricella's function of the fourth kind $F_D^{(N)}(.)$, which can be easily computed. Furthermore, we have simplified the derived expressions for various special cases such as independent and identically distributed branches, Rayleigh fading, Nakagami-*m* fading, and κ-μ fading. Additionally, a parametric study of the EVM performance of the wireless system is presented.**

***Index Terms*—Error Vector Magnitude, maximal ratio combining, η-μ fading, κ-μ fading, SIMO.**

I. Introduction

CONFORMITY with the wireless communication performance standards is an absolute necessity, when designing communication systems. Traditional approaches of quantifying a communication system's performance includes the calculation of classic metrics such as the Bit Error Ratio (BER), the throughput and the outage probability [1]–[4]. However, an alternative metric that is becoming increasingly popular is the Error Vector Magnitude (EVM) [5].

EVM as a performance metric offers several advantages. Firstly, it facilitates the identification of the specific types of degradations encountered, in addition to their particular sources in a transmission link [5]. Some of these degradations are the Inphase-Quadrature Phase (IQ) imbalance, the Local Oscillator's (LO) phase noise, carrier leakage, nonlinearity and the LO's frequency error [6], [7]. Secondly, the EVM is a symbol-level performance metric unlike the BER, which is a bit-level performance metric. Hence, EVM is more convenient for Symbol Error Rate (SER) based scenarios where multiple modulation schemes are employed, as in adaptive modulation [8]. Thirdly, it may be employed by a communication system designer for ensuring conformity with wireless standards, because EVM-based specifications have already become a part of the Wideband Code Division Multiple Access (W-CDMA) and IEEE 802.11 family of Wireless Local Area Network (WLAN) standards [5], [8]. Fourthly, in experimental studies the channel model used is often a proprietary channel, for which no closed form expressions are available either for the BER or for the EVM. In these studies, the designer has to characterize the system by transmitting and receiving bits, where the BER calculation relying on the Monte Carlo approach has a long computation time, especially at low BERs. By contrast, the EVM can be readily evaluated by transmitting fewer symbols, as compared to the BER. Hence, characterizing the performance using EVM is preferred. However, in contrast to the classic BER formulae, the current literature does not provide closed form expressions of the EVM of several important channel scenarios. Hence provides closed-form expressions for some of these important channel scenarios and partially fills this gap in the open literature. We have now added the following text to the discussions in the introduction section (please see page 2 of the revised manuscript). Moreover, EVM is easier to employ than BER as a performance metric in systems, where the transmitter requires feedback regarding the link's performance for making choices such as which adaptive modulation mode or channel coding rate to rely on. This is because employing BER would require the received signal to go through the entire receive chain before the feedback can be generated, while computation of the EVM using the received symbols would be quicker. Thus, employing EVM would be a better choice for providing real-time feedback.

In an optimized system the major source of degradation is the channel's fading [4], [9]. However, in a realistic system a range of degradations mentioned in [5] are imposed, which would play a detrimental role. Employing EVM would help the designer identify these impairments at a glance and hence to mitigate them. Mitigating the effects of these distortions would require the EVM of the the best-case scenario, where the EVM is predominantly or purely decided by the wireless channel's fading as well as by the ubiquitous receiver-noise, and not by other impairments, such as non-linear distortions and synchronization errors, etc. Hence in this paper we aim for providing the designer with closed form expressions for

Manuscript received July 21, 2015; revised December 1 2015 and February 8, 2016; accepted February 12, 2016. The financial support of the EPSRC projects EP/Noo4558/1 and EP/L018659/1, as well as of the European Research Council's Advanced Fellow Grant under the Beam-Me-Up project and of the Royal Society's Wolfson Research Merit Award is gratefully acknowledged. V. A. Thomas and S. Kumar are co-first authors. The associate editor coordinating the review of this paper and approving it for publication was T. A. Tsiftsis.

V. A. Thomas, M. El-Hajjar, and L. Hanzo are with the School of Electronics and Computer Science, University of Southampton, Southampton SO17 1BJ, U.K. (e-mail: lh@ecs.soton.ac.uk).

S. Kumar, S. Kalyani, and K. Giridhar are with the Department of Electrical Engineering, Indian Institute of Technology Madras, Chennai 600036, India.

Color versions of one or more of the figures in this paper are available online at http://ieeexplore.ieee.org.

Digital Object Identifier 10.1109/TCOMM.2016.2530797

determining this best-case target EVM. Numerous models have been employed in the literature for simulating a wireless channel [4]. Some of these models have been used for several years, including the AWGN, Rayleigh, Rician and the Nakagami-m as well as the Nakagami-q faded channels. On the other hand, recent studies are increasingly favouring the state-of-the-art η-μ and κ-μ shadowed fading channels [10], [11], because they represent all-encompassing generalizations, with the classical channels being their special cases. For example, the η-μ distribution includes the Nakagami-q (Hoyt), the Nakagami-m, the Rayleigh and the One-Sided Gaussian distribution as special cases. The κ-μ distribution includes the Nakagami-n (Rice), the Nakagami-m, the Rayleigh, and the One-Sided Gaussian distribution as special cases. The κ-μ shadowed distribution includes κ-μ and Rician shadowed distribution as special cases. Moreover, they match the experimentally measured mobile radio propagation statistics better than the other channel models [10]. The κ-μ shadowed fading is useful for modelling the satellite links. A simplified model for κ-μ fading is the shadowed-Rician fading, which has been employed for modelling the satellite links [12]–[15].

The BER, outage probability and capacity are some commonly employed performance metrics, which have been quantified for η-μ and κ-μ shadowed fading[1] channels in [16]–[19] and in the references therein. On the other hand, there is a dearth of studies that focus on the quantification of the achievable EVM for these wireless channels. Moreover, there are no studies that characterize the EVM performance for the commonly employed wireless technique of receive antenna diversity [20]. Note that a performance analysis of maximal ratio combining based receive antenna diversity was provided in [21] for the case of the shadowed-Rician fading land mobile satellite channels. Employing multiple receive antennas provides a diversity gain [20], where the link between the transmit antenna and each receive antenna is referred to as a single branch of the Single Input Multiple Output (SIMO) channel. The fading coefficients of the different branches may be independently distributed or correlated, where the branches in these scenearios are referred to as being independent or correlated, respectively. Additionally, they may have the same or different probability distribution parameters, where the branches in these scenearios are referred to as being identically or non-identically distributed, respectively. It must be noted that there is some literature on the EVM performance of the classical AWGN and Rayleigh channels for the scenario of a single receive antenna, though these are limited to only a couple of research papers. The seminal effort was made in this direction in [22], while [23] formulates the attainable EVM in an AWGN scenario. This study was extended in [24] to the scenario of non data-aided receivers communicating over both AWGN as well as Rayleigh fading channels.

A designer can compute the expected BER for various fading channels using well established formulae from the existing literature. Thus, designers have a benchmark with which they can compare the experimental results, when using BER as a performance metric. However, there are no such equivalent theoretical formulae for EVM. Hence, through this paper we aim to provide a theoretical benchmark for the EVM performance that the designer can expect in the wireless channels.

Against this background, the novel contributions of this paper may be summarised as follows:

1) We derive exact closed form expressions for the data-aided EVM[2] performance of a SIMO wireless system employing the η-μ and κ-μ shadowed fading channels and a Maximal Ratio Combining (MRC) receiver. Our expressions are derived for independent and non identically distributed branches. These results are then validated by simulations[3].
2) We also study the effect of correlated fading channels in the above-mentioned wireless system and formulate the EVM for these scenarios.
3) The expressions derived are then further simplified for various special cases, such as independent and identically distributed branches, the Rayleigh, the Nakagami and the κ-μ fading.
4) The impact of the various channel parameters such as η, μ, κ and that of the number of receive antennas N on the EVM performance is studied along with the attainable performance limits.

Our paper is organized as follows. In Section II, we present the background necessary for understanding this study, which includes discussions on the SIMO η-μ and κ-μ shadowed channel models in Section II-A and on EVM in Section II-B. Subsequently, we present our analytical characterization of the EVM performance for a SIMO wireless system in Section III, while in Section IV we provide our simulation results. Finally, we offer our conclusions in Section V.

II. Background Information

A. SIMO η-μ and κ-μ Shadowed Channel Models

For the case of a SIMO wireless channel having N receive antennas, the channel model is as follows [4]:

$$\hat{\mathbf{y}} = \mathbf{h}s + \mathbf{n}, \tag{1}$$

where s is the transmitted symbol and

$$\begin{aligned}\hat{\mathbf{y}} &= [\hat{y}_1 \ \ \hat{y}_2 \ \ \cdots \ \ \hat{y}_N]^T\\ \mathbf{h} &= [a_1 e^{j\theta_1} \ \ a_2 e^{j\theta_2} \ \ \cdots \ \ a_N e^{j\theta_N}]^T\\ \mathbf{n} &= [n_1 \ \ n_2 \ \ \cdots \ \ n_N]^T.\end{aligned} \tag{2}$$

Here $\hat{y}_k$ is the symbol received by the k^{th} receive antenna after being subjected to the multiplicative fading of $a_k e^{j\theta_k}$ and to corruption by the additive noise of n_k. In the above discussions a_k, θ_k and n_k are random variables (RVs), whose pdf has to be experimentally characterized. Typically the noise is modelled by a zero-mean Gaussian distribution, while the phase of

[1] The probability distribution function (pdf) of the sum of the squared κ-μ shadowed random variables with independent and correlated shadowing components are derived in [11] and [16], respectively. Note that the pdf derived in [11] is a special case of the pdf derived in [16].

[2] Note that data-aided EVM refers to the EVM obtained using data-aided receivers, i.e receivers which have exact knowledge of the transmitted bits.

[3] Please note that if any other detector than the MRC is used, then the EVM analysis will change significantly.

the fading co-efficient is assumed to have a uniform distribution within $[0, 2\pi]$ [4]. However, modelling the distribution of a_k or alternatively that of $X_k \propto a_k^2$ is much more challenging due to its heavy dependence on the exact nature of the wireless channel. *Note that X_k is referred to as the fading power.*

Recently η-μ and κ-μ shadowed pdfs were proposed in [10] and [11], respectively. Mathematically, the η-μ fading power (or fading attenuation) pdf is expressed as follows for each X_k [10], [25]:

$$f_{X_k,\eta-\mu}(x) = \frac{2\sqrt{\pi}\mu_k^{\mu_k+\frac{1}{2}} h_k^{\mu_k}}{\Gamma(\mu_k) H_k^{\mu_k-\frac{1}{2}} \bar{x}_k^{\mu_k+\frac{1}{2}}} x^{\mu_k-\frac{1}{2}} e^{\frac{-2\mu_k h_k x}{\bar{x}_k}} \times I_{\mu_k-\frac{1}{2}}\left(\frac{2\mu_k H_k x}{\bar{x}_k}\right), \quad (3)$$

where the modified Bessel function of the first kind of order b is represented by $I_b(.)$ and the Gamma function is denoted by $\Gamma(.)$ [10]. Here we have $\mu_k = \frac{E^2\{X_k\}}{2\text{var}\{X_k\}}[1 + (\frac{H_k}{h_k})^2]$, where $E\{.\}$ and var$\{.\}$ denote the expectation and variance, respectively and $\bar{x}_k = E\{X_k\}$ [25]. The parameters H_k and h_k may be defined in two unique ways that correspond to two distinct fading formats, where the difference arises from the physical interpretation of the parameter η_k [10][4]. In format 1, $0 < \eta_k < \infty$ is the power ratio of the in-phase and quadrature phase components of the fading signal in each multipath cluster, while H_k and h_k are given by:

$$H_k = \frac{\eta_k^{-1} - \eta_k}{4} \text{ and } h_k = \frac{2 + \eta_k^{-1} + \eta_k}{4}. \quad (4)$$

Moreover, in format 1, the η-μ power distribution is symmetrical around $\eta_k = 1$. The second format can be obtained from the first one using the relationship of $\eta_{\text{format2}} = \frac{1-\eta_{\text{format1}}}{1+\eta_{\text{format1}}}$ [10].

On the other hand, the κ-μ shadowed power pdf is expressed as follows for each X_k [11]:

$$f_{X_k,\kappa_k-\mu_k sh}(x) = \frac{\mu_k^{\mu_k} m_k^{m_k}(1+\kappa_k)^{\mu_k} x^{\mu_k-1}}{\Gamma(\mu_k)(\bar{x}_k)^{\mu_k}(\mu_k\kappa_k + m_k)^{m_k}} \times e^{-\frac{\mu_k(1+\kappa_k)x}{\bar{x}_k}} {}_1F_1\left(m_k, \mu_k, \frac{\mu_k^2\kappa_k(1+\kappa_k)}{\mu_k\kappa_k + m_k}\frac{x}{\bar{x}_k}\right), \quad (5)$$

where $\kappa_k > 0$ denotes the ratio of the total power of the dominant components to that of the scattered waves and m_k is the shadowing parmeter. In (5), $\mu_k = \frac{E^2\{X_k\}}{var\{X_k\}}\frac{1+2\kappa_k}{(1+\kappa_k)^2}$ and $\bar{x} = E\{X_k\}$, while ${}_1F_1$ is the Kummer Hypergeometric function.

The elements a_k for $1 \le k \le N$ have two important characteristics, which are as follows [4]:

1) *Similarity:* For a particular distribution model, the coefficients a_k may or may not be identically distributed. Specifically, for the cases of the η-μ and κ-μ shadowed distributions, they may or may not all have the same $\{\eta_k, \mu_k\}$ and $\{\kappa_k, \mu_k, m_k\}$ parameters, respectively.

[4]It is important to note that the η-μ pdf well models the small-scale variations of the fading signal in a scenario of non-line-of-sight communication [10].

2) *Correlation:* For a particular distribution model, the coefficients a_k associated with $1 \le k \le N$ may or may not be correlated with each other. The level of correlation is represented by the correlation matrix as follows:

$$\mathbf{C_m} = \begin{bmatrix} \rho_{11} & \rho_{12} & \cdots & \rho_{1j} & \cdots & \rho_{1N} \\ \vdots & \vdots & \vdots & \rho_{ij} & \vdots & \vdots \\ \rho_{N1} & \rho_{N2} & \cdots & \rho_{1j} & \cdots & \rho_{NN} \end{bmatrix}, \quad (6)$$

where ρ_{ij} denote the correlation coefficient between a_i and a_j. Note that $\mathbf{C_m}$ is an identity matrix for the case of all fading magnitudes being independent.

In our study, we employ Maximal Ratio Combining (MRC) [4] detection, because its performance closely matches the performance of the optimal maximum-likelihood detection [4], while its complexity is much lower. Assuming perfect channel estimation, the received symbol y after MRC is as follows:

$$y = \frac{\mathbf{h}^H \hat{\mathbf{y}}}{\mathbf{h}^H \mathbf{h}}. \quad (7)$$

B. Error Vector Magnitude

The error vector between the transmitted complex-valued symbol $s(l) = s_I(l) + j \cdot s_Q(l)$ and the received symbol $y(l) = y_I(l) + j \cdot y_Q(l)$ is defined as $e(l) = y(l) - s(l)$. Fig. 1 shows a vectorial representation of e using the constellation diagram of the communication system. The EVM of the communication system is proportional to the root mean square value of the error signal $e(l)$. In other words, if a total of L symbols are transmitted over the wireless channel, then the EVM of the SIMO system described in Section II-A may be expressed as follows [24]:

$$EVM = \sqrt{\frac{\frac{1}{L}\sum_{l=1}^{L}|y(l) - s(l)|^2}{P_o}}, \quad (8)$$

where P_o is the average symbol power. If $s(l) \in \{S_1, S_2, \cdots S_M\}$, and if all symbols are equi-probable, then P_o may be expressed as:

$$P_o = \frac{\sum_{m=1}^{M}|S_m|^2}{M}. \quad (9)$$

III. Analytical Study of the EVM for SIMO Channels

The EVM in an AWGN SISO channel has been formulated as follows for the case of data-aided receivers [23]:

$$\text{EVM} = \sqrt{\frac{1}{SNR_{SISO}}} \text{ when } L \to \infty, \quad (10)$$

where SNR_{SISO} is the channel's signal-to-noise-ratio at the single receive antenna, L is the number of symbols transmitted over the wireless channel and M is the number of unique wireless symbols in the modulation scheme.

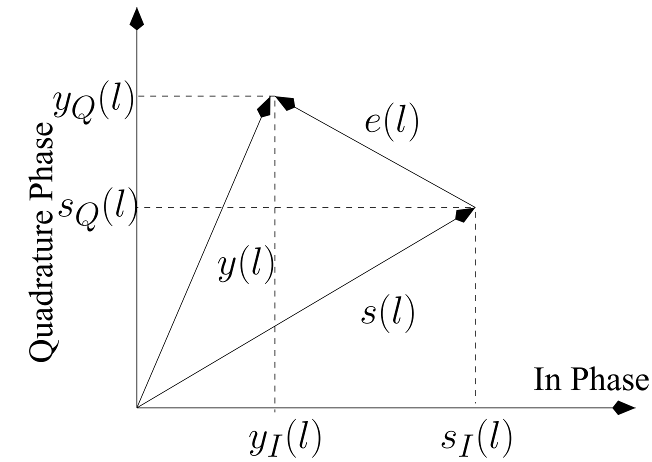

Fig. 1. Vector representation of the error between symbols s and y.

In the SIMO scenario, if we assume that the average signal to noise ratio at each receive antenna is $\gamma_i = \gamma$, then the instantaneous equivalent signal-to-noise-ratio of the overall SIMO system is [4], [24]:

$$\gamma_{inst} = \sum_{k=1}^{N} a_k^2 \gamma = N\gamma \times \frac{1}{N}\sum_{k=1}^{N} a_k^2 = SNR_{SIMO} \times Z, \quad (11)$$

where $SNR_{SIMO} = N\gamma$ is the average equivalent signal-to-noise-ratio of the overall SIMO system, which represents the power gain of using a higher number of receivers[5]. On the other hand, in (11), $Z = \frac{1}{N}\sum_{k=1}^{N} a_k^2$ is the diversity gain, which converges to 1 as the number of antennas increases (assuming each of the channel gains is normalized to have unit variance) and it hence helps overcome fading [9, P. 72]. In our simulations, we compare the EVM obtained in a SIMO channel to that of the SISO channel. Our goal is to study the diversity gain obtained by employing multiple receive antennas and not the power gain. Hence, we compare the SIMO channel to an equivalent SISO AWGN channel having a signal-to-noise-ratio of $SNR_{SISO} = SNR_{SIMO} = N\gamma$ in order to ensure the same average received power in both scenarios. Note that the BER or EVM performance of the SIMO system may be better than that of a SISO AWGN channel having an $SNR_{SISO} = \gamma$, but will always be worse than that of a SISO AWGN channel having an $SNR_{SISO} = SNR_{SIMO} = N\gamma$.

Now, employing the instantaneous SNR in (10) we obtain the instantaneous EVM to be $\text{EVM}(z) = \sqrt{\frac{1}{SNR_{SIMO} \times z}}$ for $L \to \infty$, where EVM(z) is the instantaneous EVM for the scenario of the diversity gain $Z = z$. The average EVM is formulated by employing the definition in [24] where, the average EVM is calculated by averaging over all possible values of z using the following expression:

$$\text{EVM} = \int_0^{\infty} \text{EVM}(z) f_Z(z) \text{d}z, \quad (12)$$

[5]We employ the notation SNR_{SIMO} for distinguishing between the power gain and diversity gain obtained by employing multiple receive antennas.

where $f_Z(z)$ is the pdf of Z. Let us now derive the exact closed-form expressions for the EVM in a SIMO channel, while considering two fading scenarios, namely the η-μ and κ-μ shadowed fading channels.

A. η-μ Fading SIMO Channel

In order to derive the EVM for η-μ fading, we first have to derive the pdf of $Z = \sum_{k=1}^{N} X_k$, where we have $X_k = \frac{1}{N}a_k^2$. Thus, each X_k has the pdf given in (3) with $\bar{x}_k = E\{X_k\} = \frac{1}{N}$ and the distribution parameters of $\{\eta_k, \mu_k\}$. The moment generating function (MGF) for X_k has been derived in [26]. In [27], it has been shown that the MGF of X_k can be represented as the product of the MGFs of two gamma distributed RVs (RVs), where both these gamma RVs have the same shape parameter $\alpha_{2k-1} = \alpha_{2k} = \mu_k$, but different scale parameters of $\theta_{2k-1} = \frac{\bar{x}_k}{2\mu_k(h_k+H_k)}$ and $\theta_{2k} = \frac{\bar{x}_k}{2\mu_k(h_k-H_k)}$. Using this relationship, as well as the studies in [27] and [28], we can state that $X_k = P_k + Q_k$, such that $P_k \sim \mathcal{G}(\alpha_{2k-1}, \theta_{2k-1})$, and $Q_k \sim \mathcal{G}(\alpha_{2k}, \theta_{2k})$. Note that $\mathcal{G}(\alpha_{2k}, \theta_{2k})$ denote the gamma distribution with shape parameter α_{2k} and scale parameter θ_{2k}. Thus, the sum of N η-μ RVs may be alternatively expressed as the sum of $L = 2N$ Gamma RVs, where the pdf of the sum of L Gamma RVs has been derived in [29]. Now, as stated earlier, the pdf of $Z = \sum_{k=1}^{N} X_k$ has been derived to be the following using the pdf of the sum of $2N$ Gamma RVs [29]:

$$f_{Z,\eta-\mu}(z) = \frac{z^{\sum_{i=1}^{2N}\alpha_i - 1}}{\prod_{i=1}^{2N}(\theta_i)^{\alpha_i}\,\Gamma\left(\sum_{i=1}^{2N}\alpha_i\right)} \Phi_2^{(2N)}\left(\alpha_1, \cdots, \alpha_{2N}; \sum_{i=1}^{2N}\alpha_i; \frac{-z}{\theta_1}, \cdots, \frac{-z}{\theta_{2N}}\right), \quad (13)$$

where $\Phi_2^{(N)}(.)$ is the confluent Lauricella function [30]. We can now substitute this $f_{Z,\eta-\mu}(z)$ into (12) for formulating the average EVM.

1) EVM of η-μ SIMO Channel With Independent and Nonidentically Distributed Branches:

Lemma 1: The EVM expression of the η-μ fading SIMO channel having independent and non-identically distributed (i.n.i.d) branches is given by

$$EVM_{\eta-\mu,i.n.i.d} = \frac{\sqrt{N\mu_1(1+\eta_1^{-1})}}{\sqrt{SNR_{SIMO}}} \frac{\Gamma(2\sum_{i=1}^{N}\mu_i - 0.5)}{\Gamma(2\sum_{i=1}^{N}\mu_i)} \times F_D^{(2N-1)}\Bigg[0.5, \mu_1, \mu_2, \mu_2, \cdots, \mu_N, \mu_N; 2\sum_{i=1}^{N}\mu_i; 1-\frac{1}{\eta_1}, 1-\frac{\mu_1(1+\eta_1^{-1})}{\mu_2(1+\eta_2^{-1})}, 1-\frac{\mu_1(1+\eta_1^{-1})}{\mu_2(1+\eta_2)}\cdots 1-\frac{\mu_1(1+\eta_1^{-1})}{\mu_N(1+\eta_N^{-1})}, 1-\frac{\mu_1(1+\eta_1^{-1})}{\mu_N(1+\eta_N)}\Bigg] \quad (14)$$

for $2\sum_{i=1}^{N}\mu_i > 0.5$.

Proof: See Appendix I for the proof. ■

The expression of the EVM for the i.n.i.d case is given in terms of Lauricella's function of the fourth kind $F_D^{(N)}[.]$ [30]. The function $F_D^{(N)}[a, b_1, \cdots, b_N; c; x_1, \cdots, x_N]$ can be evaluated using the following single integral expression:

$$\frac{\Gamma(c)}{\Gamma(a)\Gamma(c-a)}\int_0^1 t^{a-1}(1-t)^{c-a-1}\prod_{i=1}^{N}(1-x_i t)^{-b_i}\,\mathrm{d}t,$$
$$\text{where } \mathrm{Real}(c) > \mathrm{Real}(a) > 0, \quad (15)$$

where Real(.) returns the real part of the argument. Note that the condition $\mathrm{Real}(c) > \mathrm{Real}(a) > 0$ is satisfied by Lauricella's function of the fourth kind $F_D^{(N)}[.]$, which appeared in (14).

Special Case 1: Now, we simplify the expression in (14) for the case of independent and identically distributed (i.i.d) fading SIMO channels. Substituting both $\eta_i = \eta$ and $\mu_i = \mu\ \forall i$ into (14) and then using the following identity:

$$F_D^{(N)}[a, b_1, \cdots b_n; c, x, \cdots, x] = 2F_1[a, b_1 + \cdots + b_N; c; x], \quad (16)$$

where ${}_2F_1[.]$ is the Gauss hypergeometric function [30], we obtain,

$$\mathrm{EVM}_{\eta-\mu,i.i.d} = \frac{\sqrt{N\mu(1+\eta^{-1})}}{\sqrt{SNR_{SIMO}}}\frac{\Gamma(2N\mu-0.5)}{\Gamma(2N\mu)}$$
$${}_2F_1[0.5, N\mu; 2N\mu; 1-\frac{1}{\eta}] \text{ for } 2N\mu > 0.5. \quad (17)$$

In the following, we show that the expression shown in (17) converges to the EVM expression of AWGN channel. Note that when fading parameters $\eta = 1$ and μ tends to infinity, the η-μ channel should converge to an AWGN channel. By substituting $\eta = 1$ and $\mu \to \infty$ in (17), it can be simplified to

$$\mathrm{EVM}_{AWGN} = \lim_{\mu\to\infty}\frac{\sqrt{2N\mu}}{\sqrt{SNR_{SIMO}}}\frac{\Gamma(2N\mu-0.5)}{\Gamma(2N\mu)} = \frac{1}{\sqrt{SNR_{SIMO}}}. \quad (18)$$

This simplification follows from the fact that ${}_2F_1[0.5, N\mu; 2N\mu; 0] = 1$. We now provide the upper bound of the EVM expression given in (17) so that the impact of fading parameter η can be shown. Using the transformation ${}_2F_1[a, b; c; z] = (1-z)_2^{c-a-b}F_1[c-a, c-b; c; z]$, we obtain:

$$\mathrm{EVM}_{\eta-\mu,i.i.d} = \frac{\sqrt{N\mu(1+\eta^{-1})}}{\sqrt{SNR_{SIMO}}}\frac{\Gamma(2N\mu-0.5)}{\Gamma(2N\mu)}$$
$${}_2F_1[2N\mu-0.5, N\mu; 2N\mu; 1-\frac{1}{\eta}]\left(\frac{1}{\eta}\right)^{\mu-0.5}, \quad (19)$$

and using the bound ${}_2F_1[2N\mu-0.5, N\mu; 2N\mu; 1-\frac{1}{\eta}] <_2 F_1[2N\mu, N\mu; 2N\mu; 1-\frac{1}{\eta}]\left(\frac{1}{\eta}\right)^{-\mu}$, the expression given in (19) can be upper bounded as:

$$\mathrm{EVM}_{\eta-\mu,i.i.d} < \frac{\sqrt{N\mu(1+\eta^{-1})}}{\sqrt{SNR_{SIMO}}}\frac{\Gamma(2N\mu-0.5)}{\Gamma(2N\mu)}\left(\frac{1}{\eta}\right)^{-0.5}$$
$$= \frac{\sqrt{N\mu(1+\eta)}}{\sqrt{SNR_{SIMO}}}\frac{\Gamma(2N\mu-0.5)}{\Gamma(2N\mu)}. \quad (20)$$

Hence, it is apparent from (20) that as η increases, the EVM increases. Recall that η is the scattered-wave power ratio between the in-phase and quadrature components of each cluster of multipath and hence the EVM will be minimum when the power of the in-phase and the quadrature components is equal.

Special Case 2: The Nakagami-m fading is a special case of the η-μ fading associated with $\eta = 1$ and $2\mu = m'$. Note that m' is the shape parameter of the Nakagami-*m* fading. Substituting $\eta = 1$ and $2\mu = m$ in (14) and (17), we obtain the following expressions for the i.n.i.d and i.i.d scenarios, respectively:

$$\mathrm{EVM}_{n,i.n.i.d} = \frac{\sqrt{Nm_1'}}{\sqrt{SNR_{SIMO}}}\frac{\Gamma(\sum_{i=1}^{N} m_i' - 0.5)}{\Gamma(\sum_{i=1}^{N} m_i')}\times$$
$$F_D^{(N-1)}\left[0.5, m_2', \cdots, m_N'; \sum_{i=1}^{N} m_i'; 1-\frac{m_1'}{m_2'}, \cdots, 1-\frac{m_1'}{m_N'}\right]$$
$$\text{for } \sum_{i=1}^{N} m_i' > 0.5 \text{ and} \quad (21)$$

$$\mathrm{EVM}_{n,i.i.d} = \frac{\sqrt{Nm'}}{\sqrt{SNR_{SIMO}}}\frac{\Gamma(Nm'-0.5)}{\Gamma(Nm')} \text{ for } Nm' > 0.5. \quad (22)$$

Using the following identity from [31]:

$$\frac{\Gamma(n+a)}{\Gamma(n+b)} = n^{a-b}\left(1 + \frac{(a-b)(a+b-1)}{2n} + O(|n|^{-2})\right)$$
$$\text{for large } n, \quad (23)$$

the EVM of the i.i.d Nakagami-m scenario can be further simplified to

$$\mathrm{EVM}_{n,i.i.d} = \frac{1}{\sqrt{SNR_{SIMO}}}\left(1 + \frac{0.75}{2Nm'} + O(|Nm'|^{-2})\right)$$
$$\text{for large } Nm'. \quad (24)$$

Note that the first term in (24) represents the EVM of an AWGN channel, while the remaining terms in (24) represent the contribution of the fading. We know that as the parameter m decreases, the impact of fading becomes more severe, which is confirmed by (24). A second point that may be noted from (24) is that the EVM approaches that of an AWGN channel, when the number of receive antennas tends to infinity and/or when the fading parameter tends to infinity.

2) EVM of η-μ SIMO Channel With Correlated and Identically Distributed Branches:

Lemma 2: The EVM expression of a correlated η-μ SIMO channel associated with an MRC-based receiver is given by:

$$\mathrm{EVM}_{\eta-\mu,corr} = \frac{1}{\sqrt{\hat{\theta}_1 SNR_{SIMO}}} \frac{\Gamma(2N\mu_c - 0.5)}{\Gamma(2N\mu_c)} \times F_D^{(2N-1)}\left(0.5, \mu_c, \cdots, \mu_c; 2N\mu_c; 1 - \frac{\hat{\theta}_2}{\hat{\theta}_1}, \cdots 1 - \frac{\hat{\theta}_{2N}}{\hat{\theta}_1}\right) \quad for\ 2N\mu_c > 0.5. \tag{25}$$

Proof: See Appendix II for the proof. ■

B. κ-μ Shadowed Fading SIMO Channel

In order to derive the EVM of a κ-μ shadowed faded channel, we first have to derive the pdf of $Z = \sum_{k=1}^{N} X_k$, where $X_k = \frac{1}{N} a_k^2$. Thus, each X_k has the pdf given in (5) with $\bar{x}_k = \frac{1}{N}$ and distribution parameters of $\{\kappa_k, \mu_k, m_k\}$. The pdf of Z has been shown in [11] to be as follows:

$$f_{Z,\kappa-\mu sh}(z) = \prod_{i=1}^{N} \frac{\mu_i^{\mu_i} m_i^{m_i} (1+\kappa_i)^{\mu_i} z^{\sum_{i=1}^{N} \mu_i - 1}}{\Gamma(\sum_{i=1}^{N} \mu_i)(\mu_i \kappa_i + m_i)^{m_i} \bar{x}_i^{\mu_i}} \cdot \Phi_2^{(N)}\left(\mu_1 - m_1, \cdots \mu_N - m_N, m_1 \cdots m_n; \sum_{i=1}^{N} \mu_i; -\frac{\mu_1(1+\kappa_1) z}{\bar{x}_1}, \cdots, -\frac{\mu_N(1+\kappa_N) z}{\bar{x}_N}, -\frac{\mu_1 m_1 (1+\kappa_1) z}{(\mu_1\kappa_1 + m_1)\bar{x}_1} \cdots - \frac{\mu_N m_N (1+\kappa_N) z}{(\mu_N \kappa_N + m_N)\bar{x}_N}\right). \tag{26}$$

We can now substitute $f_{Z,\kappa-\mu sh}(z)$ in (12) to obtain the average EVM.

1) EVM of κ-μ Shadowed Fading SIMO Channel With i.n.i.d Branches:

Lemma 3: The EVM expression of κ-μ shadowed fading SIMO channel having i.n.i.d branches is given by

$$EVM_{\kappa-\mu sh,i.n.i.d} = \frac{\sqrt{N\mu_1(1+\kappa_1)}}{\sqrt{SNR_{SIMO}}} \frac{\Gamma\left(\sum_{i=1}^{N}\mu_i - 0.5\right)}{\Gamma\left(\sum_{i=1}^{N}\mu_i\right)} F_D^{(2N-1)}\Bigg(0.5, \mu_2 - m_2, \cdots, \mu_2 - m_2, m_1, \cdots m_N; \sum_{i=1}^{N}\mu_i; 1 - \frac{\mu_1(1+\kappa_1)}{\mu_2(1+\kappa_2)}, \cdots, 1 - \frac{\mu_1(1+\kappa_1)}{\mu_N(1+\kappa_N)}, 1 - \frac{(\mu_1\kappa_1 + m_1)}{m_1} \cdots 1 - \frac{(\mu_N\kappa_N + m_N)\mu_1(1+\kappa_1)}{m_N \mu_N (1+\kappa_N)}\Bigg), \quad for \sum_{i=1}^{N}\mu_i > 0.5. \tag{27}$$

Proof: See Appendix III for the proof. ■

Special Case 1: Now, we simplify the expression in (27) for the i.i.d scenario, where we set $\mu_i = \mu$ and $\kappa_i = \kappa\ \forall i$ to obtain:

$$\mathrm{EVM}_{\kappa-\mu sh,i.i.d} = \frac{\sqrt{N\mu(1+\kappa)}}{\sqrt{SNR_{SIMO}}} \frac{\Gamma(N\mu - 0.5)}{\Gamma(N\mu)} {}_2F_1[0.5, Nm; , N\mu; -\frac{\mu\kappa}{m}] \text{ for } N\mu > 0.5. \tag{28}$$

In the following, we will show that the above expression converges to the EVM expression of AWGN channel. Note that when fading parameters $\kappa = 0$ and μ tends to infinity, the κ-μ channel should converge to an AWGN channel. By putting $\kappa = 0$ and $\mu \to \infty$ the above expression can be simplified to

$$\mathrm{EVM}_{AWGN} = \lim_{\mu\to\infty} \frac{\sqrt{N\mu}}{\sqrt{SNR_{SIMO}}} \frac{\Gamma(N\mu - 0.5)}{\Gamma(N\mu)} = \frac{1}{\sqrt{SNR_{SIMO}}}. \tag{29}$$

The above simplification follows from the fact that ${}_2F_1[0.5, N\mu; 2N\mu; 0] = 1$. Note that the EVM expression for an κ-μ shadowed channel converges to the expression of AWGN channel when fading parameter $\kappa = 0$ and μ tends to infinity, as expected.

Special Case 2: We now derive the closed-form expression of EVM for the κ-μ fading SIMO channel having i.i.d branches. Note that the κ-μ fading is a special case of the κ-μ shadowed fading with $m \to \infty$. Using the following identity [32]:

$$\lim_{b\to\infty} {}_2F_1\left[a, b, c, \frac{z}{b}\right] = {}_1F_1[a, c, z], \tag{30}$$

the ${}_2F_1[.]$ given in (28) can be simplified for $m \to \infty$ as follows:

$${}_2F_1[0.5, Nm; , N\mu; , -\frac{\mu\kappa}{m}] = 1F_1[0.5; N\mu; -N\mu\kappa], \tag{31}$$

where ${}_1F_1[.]$ is the Kummer hypergeometric function [30]. Therefore, the EVM expression of the κ-μ fading SIMO channel having i.i.d branches is given by

$$\mathrm{EVM}_{\kappa-\mu,i.i.d} = \frac{\sqrt{N\mu(1+\kappa)}}{\sqrt{SNR_{SIMO}}} \frac{\Gamma(N\mu - 0.5)}{\Gamma(N\mu)} {}_1F_1(0.5, N\mu, -N\mu\kappa) \text{ for } N\mu > 0.5. \tag{32}$$

The EVM expression of the κ-μ fading SISO channel is given by

$$\mathrm{EVM}_{\kappa-\mu} = \frac{\sqrt{\mu(1+\kappa)}}{\sqrt{SNR}} \frac{\Gamma(\mu - 0.5)}{\Gamma(\mu)} 1F_1(0.5, \mu, -\mu\kappa) \quad \text{for } \mu > 0.5. \tag{33}$$

Additional validation of Equation (33): In the following, we derive the EVM expression of the κ-μ fading SISO channel using the negative moment given in [10] in order to further validate our derivations[6]. The EVM for κ-μ channel is

[6]Note that the negative moment of sum of generalized fading distribution is not available and hence we cannot derive the EVM expression for SIMO channel.

given by

$$\mathrm{EVM}_{\kappa-\mu} = \int_{a=0}^{\infty} \sqrt{\frac{1}{a^2 \mathrm{SNR}}}\, f_{\kappa-\mu}(a)\mathrm{d}a$$

where $f_{\kappa-\mu}(a)$ is the κ-μ envelope probability density function. It is apparent from the above expression that the $\mathrm{EVM}_{\kappa-\mu}$ is the negative moment of the κ-μ fading distribution. Using the moment expression given in [10], the $\mathrm{EVM}_{\kappa-\mu}$ can be obtained as

$$\mathrm{EVM}_{\kappa-\mu} = \frac{\sqrt{\mu(1+\kappa)}}{\sqrt{SNR}} \frac{\Gamma(\mu-0.5)\,\exp(-\kappa\mu)}{\Gamma(\mu)} \\ {}_1F_1(\mu-0.5, \mu, \mu\kappa) \text{ for } \mu > 0.5. \quad (34)$$

Then, using the transformation $e_1^{-z} F_1(b-a, b, z) = 1F_1(a, b, -z)$, we can simplify the above expression to

$$\mathrm{EVM}_{\kappa-\mu} = \frac{\sqrt{\mu(1+\kappa)}}{\sqrt{SNR}} \frac{\Gamma(\mu-0.5)}{\Gamma(\mu)} 1F_1(0.5, \mu, -\mu\kappa). \quad (35)$$

Therefore, we have shown that the expressions given in (35) and (33) are same. Note that the functional form of the pdf of the sum of correlated κ-μ shadowed random variables is similar to that of the sum of correlated η-μ random variables. Hence, the EVM expression for a correlated κ-μ shadowed SIMO channel can be derived in a similar manner to that of the η-μ SIMO channel. Furthermore, κ-μ fading is a special case of κ-μ shadowed fading and hence the EVM can be obtained numerically by employing a very high value of m in the EVM expression for a κ-μ shadowed fading channel.

IV. Simulation Results

In order to validate the EVM expressions derived for η-μ and κ-μ shadowed fading channels associated with the arbitary parameters, we simulated a BPSK modulation-based system communicating over these channels. We implemented a simulation-based solution of (12) using 1 transmit and N receive antennas. The simulations employed the Monte Carlo approach, which relies on transmitting a large number of bits over the wireless channel and computing the average EVM. The simulations were carried out in Matlab.

Fig. 2 shows the EVM variation with respect to SNR_{SIMO} for the case of SIMO channels having independent and non-identically distributed branches, where it can be seen that the simulation results closely match the theoretical values.

Fig. 3 depicts the variation of EVM with respect to SNR_{SIMO} for η-μ fading. Here, we have considered $N = 3$ and $\eta \geq 1$, since η is symmetrical about 1. Firstly, it may be seen that the analytical results match with the simulation results for the entire range of SNR_{SIMO}. Secondly, it may be observed that as η increases, the EVM also increases for a fixed value of μ. Recall that η is the power ratio of the in-phase and quadrature-phase components of the fading signal in each multipath cluster. Hence, as the power ratio of the in-phase and

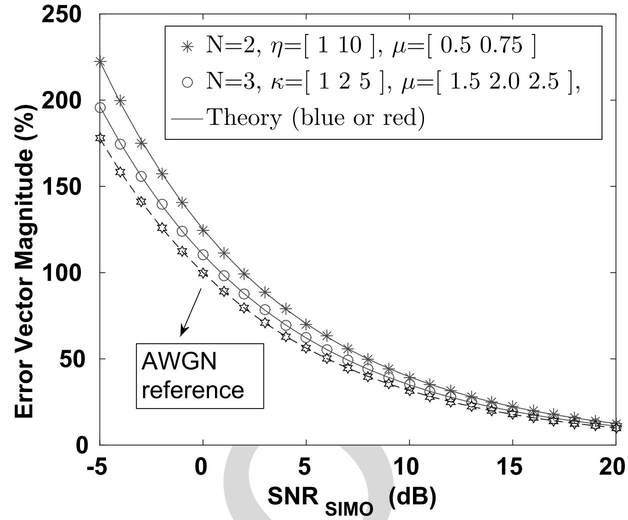

Fig. 2. The EVM for η-μ and κ-μ shadowed i.n.i.d SIMO channels.

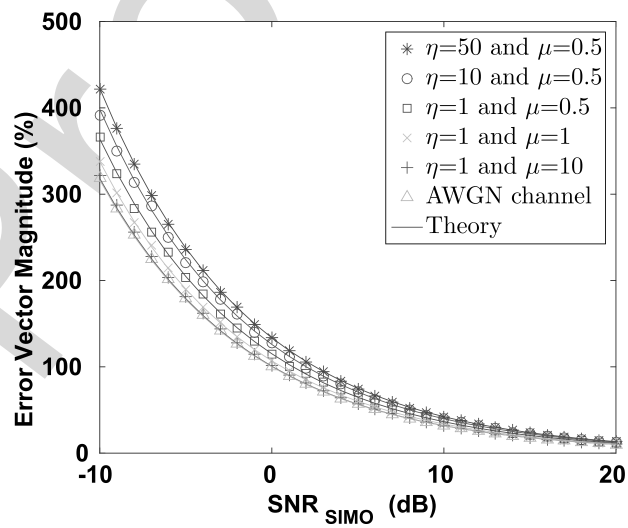

Fig. 3. The EVM for different values of η and μ, when $N = 3$ and the channels are i.i.d.

quadrature-phase components increases, the EVM increases. In other words, the EVM would be minimum, when the power of the in-phase and quadrature-phase components of the fading signal in each multipath cluster is equal. Thirdly, as the shape parameter μ increases, the EVM decreases and it approaches the EVM of an AWGN channel.

Fig. 4 shows the variation of EVM with respect to SNR_{SIMO} for different values of N. Firstly, observe that the simulation results closely match the analytical results. Secondly, as the number of antennas increases, the EVM decreases and it approaches the EVM of an AWGN channel. Interestingly, it may be seen that the EVM decreases significantly as the number of antennas increases from 1 to 2. However, the EVM reduction becomes less significant, as the number of antennas increases from $N = 2$ to 3 and so on.

Fig. 5 shows the variation of EVM as a function of SNR_{SIMO} for different values of correlation coefficients. The correlation between the SIMO branches is defined by the correlation matrix in (6) in conjunction with $\rho_{pq} = \rho^{|p-q|}$, where

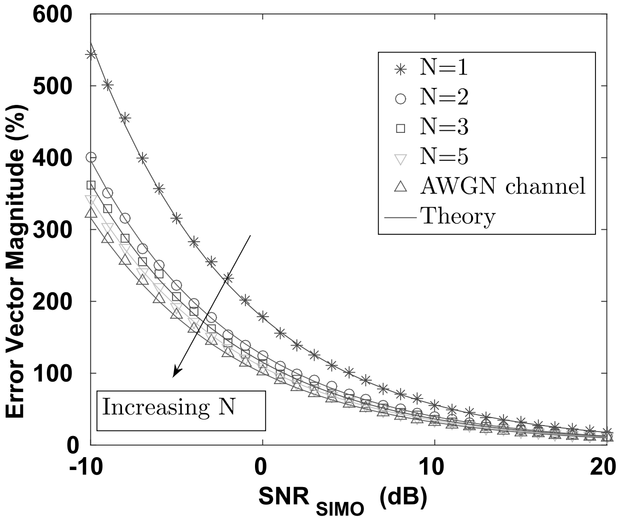

Fig. 4. The EVM for different values of N, when η = 1 and μ = 0.5 and the channels are i.i.d.

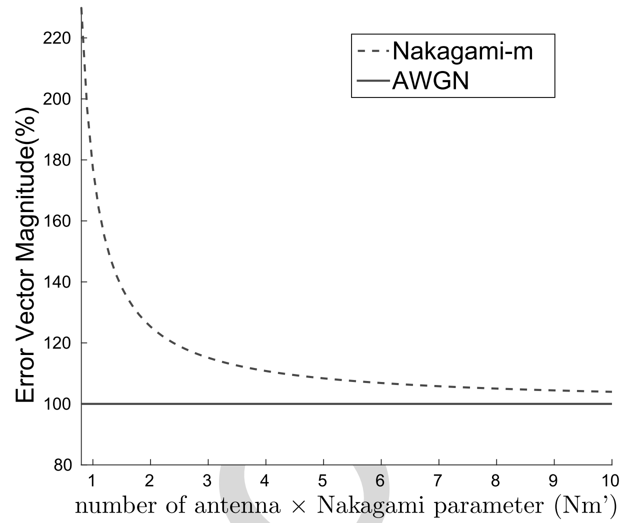

Fig. 6. Variation in EVM with respect to $N \times m'$ for a Nakagami SIMO channel which are i.i.d.

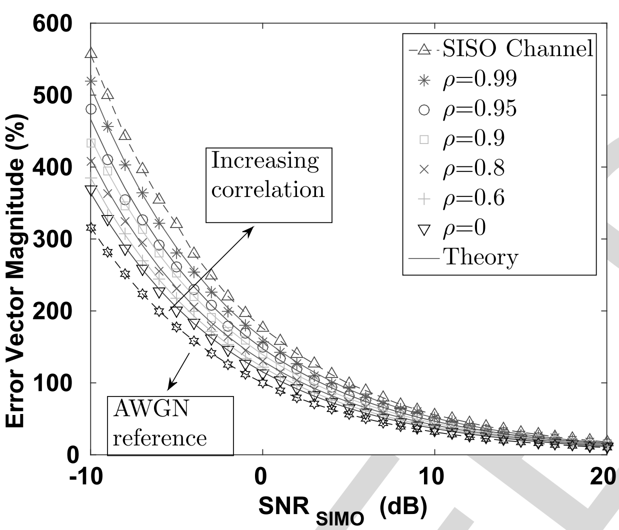

Fig. 5. The EVM for different values of correlation, when N = 3, while η = 1 and μ = 0.5 for all the channels.

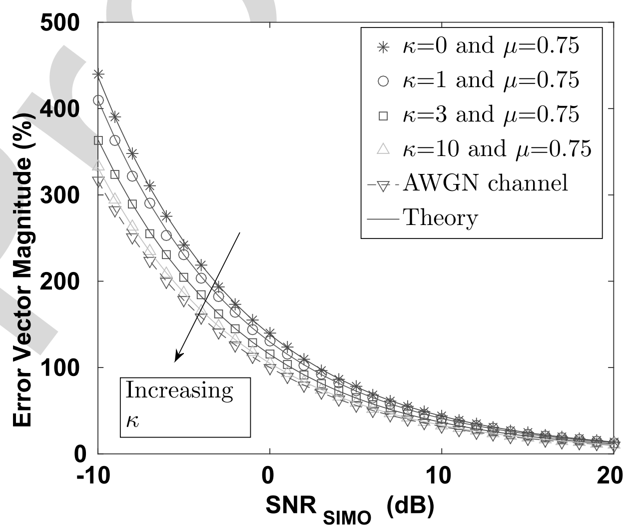

Fig. 7. The EVM for different combinations of κ and μ, when $N = 2$ and the channels are i.i.d.

we have $p, q = 1, \cdots, N$. Firstly, it may be seen that the simulation results closely match the analytical results for all values of the correlation coefficients. Secondly, it is observed that the EVM increases, as the correlation among the branches increases and it approaches the EVM of a SISO channel. Furthermore, the rate at which the EVM increases is higher, when the correlation coefficients are high.

Fig. 6 shows the variation of EVM versus the $N \times m$ product for the special case of Nakagami channels. It may be seen that the EVM decreases, as either N or m increases. Interestingly, the rate at which the EVM decreases is higher, when the number of antennas and the Nakagami-m fading parameter are small. This phenomenon may also be observed from (24), where the EVM of the Nakagami-m fading is shown to be a function of $1/(N \times m)$.

Fig. 7 shows the EVM variation versus SNR_{SIMO} for κ-μ fading. Again, the simulation results closely match the analytical results. It may be seen that as κ increases, the EVM decreases and it approaches the EVM of an AWGN channel. Recall that κ represents the ratio of the total power of the dominant components to that of the scattered waves. Hence, as the ratio of the total power of the dominant components to that of the scattered waves increases, the EVM decreases, as expected.

V. Conclusions

We have derived exact closed-form expressions for the data-aided EVM in η-μ and κ-μ shadow faded SIMO channels having independent and non-identically distributed branches. The EVM expression is also derived for the scenario of correlated SIMO branches. Furthermore, the expressions derived may be readily simplified for various special cases, such as independent and identically distributed fading, the Rayleigh, the Nakagami-m and finally the κ-μ fading. Subsequently, we performed a simulation based study of this system in order to validate the analytical results. Finally, a parametric study of the

EVM performance of the wireless communication system considered showed that as the Nakagami fading parameter m and/or the number of antennas N increases, the EVM decreases and the rate at which the EVM decreases is higher, when the fading parameter and/or the number of antennas is small.

ACKNOWLEDGMENT

We are grateful to Dr. R. A. Shafik for his valuable inputs.

APPENDIX A

The EVM for a AWGN SISO channel is given by (10) [23], [24]. Thus, the instantaneous EVM, namely $EVM(z)$, is computed using (10) but with the replacement of SNR_{SISO} with the instantaneous signal-to-noise ratio, where $zSNR_{SIMO}$ is the instantaneous signal-to-noise ratio as per (11). Thus, the EVM of a η-μ fading channel is defined as follows [24]:

$$\mathrm{EVM}_{\eta-\mu,i.n.i.d} = \int_0^\infty \mathrm{EVM}(z)\, f_{Z,\eta-\mu}(z)\mathrm{d}z, \quad (36)$$

which simply weights the AWGN channel's EVM by the specific probability of occurance of each particular instantaneous SNR given by its distribution and then averages it by integrating it across the entire instantaneous SNR range. Now substituting (13) in (36), we get:

$$\begin{aligned}\mathrm{EVM}_{\eta-\mu,i.n.i.d} &= \int_0^\infty \sqrt{\frac{1}{zSNR_{SIMO}}}\frac{z^{\sum_{i=1}^{2N}\alpha_i-1}}{\prod_{i=1}^{2N}(\theta_i)^{\alpha_i}\Gamma\left(\sum_{i=1}^{2N}\alpha_i\right)}\cdot\\ &\Phi_2^{(2N)}\left(\alpha_1,\cdots,\alpha_{2N};\sum_{i=1}^{2N}\alpha_i;\frac{-z}{\theta_1},\cdots,\frac{-z}{\theta_{2N}}\right)\mathrm{d}z\\ &= \int_0^\infty \sqrt{\frac{1}{SNR_{SIMO}}}\frac{z^{\sum_{i=1}^{2N}\alpha_i-1.5}}{\prod_{i=1}^{2N}(\theta_i)^{\alpha_i}\Gamma\left(\sum_{i=1}^{2N}\alpha_i\right)}\\ &\Phi_2^{(2N)}\left(\alpha_1,\cdots,\alpha_{2N};\sum_{i=1}^{2N}\alpha_i;\frac{-z}{\theta_1},\cdots,\frac{-z}{\theta_{2N}}\right)\mathrm{d}z. \quad (37)\end{aligned}$$

Using the transformation [30, P. 177]:

$$\begin{aligned}&e^{-x_i}\Phi_2^{(n)}(b_1,\cdots,b_n;c;x_1,\cdots,x_n)\\ &\quad=\Phi_2^{(n)}(b_1,\cdot,b_{i-1},c-b_1-\cdot-b_n,b_{i+1},\cdot,b_n;c;\\ &\quad x_1-x_i,\cdots x_{i-1}-x_i,-x_i,x_{i+1}-x_i,\cdot,x_n-x_i), \quad (38)\end{aligned}$$

the $\mathrm{EVM}_{\eta-\mu,i.n.i.d}$ can be rewritten as:

$$\begin{aligned}\mathrm{EVM}_{\eta-\mu,i.n.i.d} &= K_1\int_0^\infty z^{\sum_{i=1}^{2N}\alpha_i-1.5}e^{-\frac{z}{\theta_1}}\\ &\times\Phi_2^{(2N)}\left(0,\alpha_2,\cdots,\alpha_{2N};\sum_{i=1}^{2N}\alpha_i;\frac{z}{\theta_1},\left(\frac{1}{\theta_1}-\frac{1}{\theta_2}\right)z,\right.\\ &\left.\cdots\left(\frac{1}{\theta_1}-\frac{1}{\theta_N}\right)z\right)\mathrm{d}z, \quad (39)\end{aligned}$$

where we have $K_1=\sqrt{\frac{1}{SNR_{SIMO}}}\frac{1}{\prod_{i=1}^{2N}(\theta_i)^{\alpha_i}\Gamma\left(\sum_{i=1}^{2N}\alpha_i\right)}$. Note that if one of the numerator parameters of the series expansion of $\Phi_2^{(N)}$ goes to zero, then $\Phi_2^{(N)}$ becomes $\Phi_2^{(N-1)}$ and hence the above $\Phi_2^{(2N)}$ will become $\Phi_2^{(2N-1)}$ with appropriate parameters. Using the transformation $\frac{z}{\theta_1}=t$ we obtain:

$$\begin{aligned}\mathrm{EVM}_{\eta-\mu,i.n.i.d} &= K_1\theta_1^{\sum_{i=1}^{2N}\mu_i-0.5}\int_0^\infty t^{\sum_{i=1}^{2N}\alpha_i-1.5}e^{-t}\\ &\times\Phi_2^{(2N-1)}\left(\alpha_2,\cdots,\alpha_{2N};\sum_{i=1}^{2N}\alpha_i;\left(1-\frac{\theta_1}{\theta_2}\right)t,\right.\\ &\left.\cdots\left(1-\frac{\theta_1}{\theta_N}\right)t\right)\mathrm{d}t. \quad (40)\end{aligned}$$

Using the following identity [30, P. 51]:

$$\begin{aligned}&F_D^{(n)}[a,b_1,\cdots,b_n,c,x_1,\cdots,x_n]\\ &=\frac{1}{\Gamma(a)}\int_{t=0}^\infty e^{-t}t^{a-1}\Phi_2^{(n)}[b_1,\cdots,b_n,c,x_1t,\cdots,x_nt]\mathrm{d}t, \quad (41)\end{aligned}$$

where $\mathrm{Real}(a)>0$, one obtains:

$$\begin{aligned}\mathrm{EVM}_{\eta-\mu,i.n.i.d} &= K_1\theta_1^{\sum_{i=1}^{2N}\alpha_i-0.5}\Gamma\left(\sum_{i=1}^{2N}\alpha_i-0.5\right)\\ &\times F_D^{(2N-1)}\left(\sum_{i=1}^{2N}\alpha_i-0.5,\alpha_2,\cdots,\alpha_{2N};\sum_{i=1}^{2N}\alpha_i;\right.\\ &\left.1-\frac{\theta_1}{\theta_2},\cdots,1-\frac{\theta_1}{\theta_N}\right) \quad (42)\end{aligned}$$

for $\sum_{i=1}^{2N}\alpha_i>0.5$. Here $F_D^{(N)}[a,b_1,\cdots,b_N;c;x_1,\cdots,x_N]$ is the Lauricella's function of the fourth kind. Again, using the following identity:

$$\begin{aligned}&F_D^{(n)}[a,b_1,\cdots,b_n,c,x_1,\cdots,x_n]=\prod_{i=1}^{n}(1-x_i)^{-b_i}\\ &F_D^{(n)}[a,b_1,\cdots,b_n,c,\frac{x_1}{x_1-1},\cdots,\frac{x_n}{x_n-1}], \quad (43)\end{aligned}$$

we arrive at:

$$\begin{aligned}\mathrm{EVM}_{\eta-\mu,i.n.i.d} &= K_1\theta_1^{\sum_{i=1}^{2N}\alpha_i-0.5}\Gamma\left(\sum_{i=1}^{2N}\alpha_i-0.5\right)\prod_{i=2}^{2N}\left(\frac{\theta_1}{\theta_i}\right)^{-\alpha_i}\\ &\times F_D^{(2N-1)}\left(0.5,\alpha_2,\cdots,\alpha_{2N};\sum_{i=1}^{2N}\alpha_i;1-\frac{\theta_2}{\theta_1},\cdots,1-\frac{\theta_{2N}}{\theta_1}\right). \quad (44)\end{aligned}$$

Substituting the value of K_1, the $\mathrm{EVM}_{\eta-\mu,i.n.i.d}$ expression can be simplified to

$$\mathrm{EVM}_{\eta-\mu,i.n.i.d} = \frac{1}{\sqrt{\theta_1 SNR_{SIMO}}}\frac{\Gamma(\sum_{i=1}^{2N}\alpha_i - 0.5)}{\Gamma(\sum_{i=1}^{2N}\alpha_i)} \times F_D^{(2N-1)}\left(0.5, \alpha_2, \cdots, \alpha_{2N}; \sum_{i=1}^{2N}\alpha_i; 1-\frac{\theta_2}{\theta_1}, \cdots, 1-\frac{\theta_{2N}}{\theta_1}\right). \tag{45}$$

Substituting the value of θ_i, α_i and $\bar{z} = 1/N$ into (45), we obtain the final expression of $\mathrm{EVM}_{\eta-\mu,i.n.i.d}$ given in (14).

Appendix B

The underlying philosophy in this derivation is similar to that of an $\eta-\mu$ SIMO channel with i.n.i.d branches. We now consider the scenario studies in this paper, where Z is the sum of N correlated and identically distributed η-μ RVs X_k having distribution parameters $\{\eta_k, \mu_c\}$. Note that all the X_ks have the same μ_c but different η_k. As discussed in the first paragraph of Section III-A, an η-μ random variable may be expressed as the sum of two independent Gamma distributed RVs. It has been discussed in [28] that each X_k may be expressed as

$$X_k = P_k + Q_k, \tag{46}$$

where $P_k \sim \mathcal{G}(\mu_c, \theta_{2k-1})$, and $Q_k \sim \mathcal{G}(\mu_c, \theta_{2k})$ with $\theta_{2k-1} = \frac{\bar{x}_k}{2\mu_c(h_k+H_k)}$ and $\theta_{2k} = \frac{\bar{x}_k}{2\mu_c(h_k-H_k)}$. Similar to Section III-A, $\bar{x}_k = 1/N$, while h_k and H_k are given by (4). Note that the correlation among the different X_ks results in a correlation among the different P_ks and among the Q_ks, but there is no correlation between the P_ks and Q_ks. If ρ_{ij}^{xx} is the correlation between $X_i = P_i + Q_i$ and $X_j = P_j + Q_j$, while ρ_{ij}^{pp} and ρ_{ij}^{qq} is the correlation between $\{P_i, P_j\}$ and $\{Q_i, Q_j\}$, respectively then we have (47), shown at the bottom of the page.

In our study Z is the sum of N correlated and identically distributed η-μ RVs X_k. Employing (46), we may state that Z is the sum of $2N$ correlated and non-identically distributed Gamma distributed RVs M_i, namely $\{M_1 = P_1, M_2 = Q_1, M_3 = P_2, M_4 = Q_2 \ldots, M_{2N-1} = P_N, M_{2N} = Q_N\}$. The pdf of the sum of N correlated η-μ math RVs is given by [16], [29], [33]

$$F_{Z,\eta-\mu,corr}(z) = \frac{z^{2N\mu_c-1}}{\det(\mathbf{A})^{\mu_c}\Gamma(2N\mu_c)} \times \Phi_2^{(2N)}\left(\mu_c, \cdots, \mu_c; 2N\mu_c; \frac{-z}{\hat{\theta}_1}, \cdots, \frac{-z}{\hat{\theta}_{2N}}\right), \tag{48}$$

where $\hat{\theta}_i$ is the eigen values of $\mathbf{A} = \mathbf{DC}$ with $\mathbf{D}$ being a diagonal matrix with entries θ_i and $\det(\mathbf{A}) = \prod_{i=1}^{N}\hat{\theta}_i$ is the determinant of the matrix $\mathbf{A}$. Here, $\mathbf{C}$ is the symmetric positive definite (s.p.d) matrix and is given in (49), shown at the bottom of the page. where ρ_{ij}^{mm} denotes the correlation coefficient between M_i and M_j, and is given by,

$$\rho_{ij}^{mm} = \rho_{ji}^{mm} = \frac{\mathrm{cov}(M_i, M_j)}{\sqrt{\mathrm{var}(M_i)\mathrm{var}(M_j)}}, 0 \le \rho_{ij} \le 1, \tag{50}$$

with $\mathrm{cov}(M_i, M_j)$ being the covariance between M_i and M_j. Note that the alternate zeros are a consequence of P_ks and Q_ks being independent.

Just as in (36), the EVM of a SIMO channel encountering correlated η-μ fading and employing MRC reception is defined as follows:

$$\mathrm{EVM}_{\eta-\mu,corr} = \int_0^\infty \mathrm{EVM}(z)\ f_{Z,\eta-\mu,corr}(z)\mathrm{d}z, \tag{51}$$

The functional form of the pdf of the sum of correlated gamma RVs is similar to that of the sum of i.n.i.d. $\eta-\mu$ RVs, as given in (13). Hence the EVM expression in (51) may be readily simplified to:

$$\mathrm{EVM}_{\eta-\mu,corr} = \frac{1}{\sqrt{\hat{\theta}_1 SNR_{SIMO}}}\frac{\Gamma(2N\mu_c - 0.5)}{\Gamma(2N\mu_c)} \times F_D^{(2N-1)}\left(0.5, \mu_c, \cdots, \mu_c; 2N\mu_c; \left(1-\frac{\hat{\theta}_2}{\hat{\theta}_1}\right), \cdots \left(1-\frac{\hat{\theta}_{2N}}{\hat{\theta}_1}\right)\right) \tag{52}$$

Note that $\hat{\theta}_i$ is the eigen values of $\mathbf{A} = \mathbf{DC}$ with $\mathbf{D}$ being a diagonal matrix with entries θ_i and $\mathbf{C}$ is the symmetric positive definite (s.p.d) covariance matrix defined in (49).

$$\rho_{ij}^{xx} = \frac{\rho_{ij}^{pp}\sqrt{\mathrm{var}(P_i)\mathrm{var}(P_j)} + \rho_{ij}^{qq}\sqrt{\mathrm{var}(Q_i)\mathrm{var}(Q_j)}}{\sqrt{\mathrm{var}(P_i)\mathrm{var}(P_j) + \mathrm{var}(Q_i)\mathrm{var}(Q_j) + \mathrm{var}(P_i)\mathrm{var}(Q_j) + \mathrm{var}(P_j)\mathrm{var}(Q_i)}} \tag{47}$$

$$\mathbf{C} = \begin{bmatrix} 1 & 0 & \sqrt{\rho_{12}^{pp}} & 0 & \sqrt{\rho_{13}^{pp}} & 0 & \ldots & \sqrt{\rho_{1N}^{pp}} & 0 \\ 0 & 1 & 0 & \sqrt{\rho_{12}^{qq}} & 0 & \sqrt{\rho_{13}^{qq}} & \ldots & 0 & \sqrt{\rho_{1N}^{qq}} \\ \sqrt{\rho_{21}^{pp}} & 0 & 1 & 0 & \sqrt{\rho_{23}^{pp}} & 0 & \ldots & \sqrt{\rho_{2N}^{pp}} & 0 \\ \vdots & \vdots & \vdots & \vdots & \vdots & \vdots & \vdots & \vdots & \vdots \\ 0 & \sqrt{\rho_{N1}^{qq}} & 0 & \sqrt{\rho_{N2}^{qq}} & 0 & \sqrt{\rho_{N3}^{qq}} & \ldots & 0 & 1 \end{bmatrix}. \tag{49}$$

Appendix C

The pdf $f_{Z,\kappa-\mu sh}(z)$ is presented in (26). Assuming that $\beta_i = \frac{\bar{x}_i}{\mu_i(1+\kappa_i)}$ and $\delta_i = \frac{(\mu_i\kappa_i+m_i)\bar{x}_i}{\mu_i(1+\kappa_i)m_i}$, we can rewrite the pdf $f_{Z,\kappa-\mu sh}(z)$ as

$$f_{Z,\kappa-\mu sh}(z) = \left(\prod_{i=1}^{N} \frac{1}{\beta_i^{\mu_i-m_i}\delta_i^{m_i}}\right) \frac{z^{\sum_{i=1}^{N}\mu_i-1}}{\Gamma\left(\sum_{i=1}^{N}\mu_i\right)} \times \Phi_2^{(2N)}\left(\mu_1-m_1,\cdots,\mu_N-m_N, m_1\cdots,m_N; \sum_{i=1}^{N}\mu_i; -\frac{z}{\beta_1},\cdots,-\frac{z}{\beta_N},-\frac{z}{\delta_1},\cdots,\frac{z}{\delta_N}\right). \quad (53)$$

The EVM of κ-μ shadow fading SIMO channel with i.n.i.d branches is defined as follows [24]:

$$\mathrm{EVM}_{\kappa-\mu sh,i.n.i.d} = \int_0^\infty \mathrm{EVM}(z)\ f_{Z,\kappa-\mu sh}(z)\mathrm{d}z. \quad (54)$$

Note that the functional form of the pdf of the sum of κ-μ shadowed RVs is similar to that of the sum of η-μ RVs, as given in (13). Hence the EVM of the κ-μ shadowed fading SIMO channel with i.n.i.d branches may be expressed as follows:

$$\mathrm{EVM}_{\kappa-\mu sh,i.n.i.d} = \frac{1}{\sqrt{\beta_1 SNR_{SIMO}}} \frac{\Gamma\left(\sum_{i=1}^{N}\mu_i - 0.5\right)}{\Gamma\left(\sum_{i=1}^{N}\mu_i\right)} \times F_D^{(2N-1)}\left(0.5, \mu_2-m_2,\cdots,\mu_2-m_2, m_1,\cdots m_N; \sum_{i=1}^{N}\mu_i; 1-\frac{\beta_2}{\beta_1},\cdots,1-\frac{\beta_N}{\beta_1}, 1-\frac{\delta_1}{\beta_1}\cdots 1-\frac{\delta_N}{\beta_1}\right). \quad (55)$$

Substituting the value of β_i and δ_i and $\bar{x}_i = 1/N\ \forall i$ into (55), we obtain the final expression of $\mathrm{EVM}_{\kappa-\mu sh,i.n.i.d}$, which is given in (27).

References

[1] J. Zhang, Z. Tan, H. Wang, Q. Huang, and L. Hanzo, “The effective throughput of MISO systems over κ-μ fading channels,” *IEEE Trans. Veh. Technol.*, vol. 63, no. 2, pp. 943–947, Feb. 2014.

[2] V. Aalo, T. Piboongungon, and G. Efthymoglou, “Another look at the performance of MRC schemes in Nakagami-M fading channels with arbitrary parameters,” *IEEE Trans. Commun.*, vol. 53, no. 12, pp. 2002–2005, Dec. 2005.

[3] D. Chen, L.-L. Yang, and L. Hanzo, “Multi-hop diversity aided multi-hop communications: A cumulative distribution function aware approach,” *IEEE Trans. Commun.*, vol. 61, no. 11, pp. 4486–4499, Nov. 2013.

[4] L. Hanzo, S. X. Ng, T. Keller, and W. Webb, *Quadrature Amplitude Modulation*, 2nd ed. Hoboken, NJ, USA: Wiley, 2004.

[5] R. Vaughan, N. Scott, and D. White, “Eight hints for making and interpreting EVM measurements,” Agilent Application Note, May 2005, pp. 1–12.

[6] R. Liu, Y. Li, H. Chen, and Z. Wang, “EVM estimation by analyzing transmitter imperfections mathematically and graphically,” *Analog Integr. Circuits Signal Process.*, vol. 48, no. 3, pp. 257–262, Jan. 2014.

[7] A. Georgiadis, “Gain, phase imbalance, and phase noise effects on error vector magnitude,” *IEEE Trans. Veh. Technol.*, vol. 53, no. 2, pp. 443–449, Mar. 2004.

[8] R. Shafik, S. Rahman, R. Islam, and N. Ashraf, “On the error vector magnitude as a performance metric and comparative analysis,” in *Proc. Int. Conf. Emerg. Technol. (ICET)*, Nov 2006, pp. 27–31.

[9] D. Tse and P. Viswanath, *Fundamentals of Wireless Communication*. Cambridge, U.K.: Cambridge Univ. Press, 2005.

[10] M. D. Yacoub, “The κ-μ distribution and the η-μ distribution,” *IEEE Antennas Propag. Mag.*, vol. 49, no. 1, pp. 68–81, Feb. 2007.

[11] J. Paris, “Statistical characterization of κ-μ shadowed fading,” *IEEE Trans. Veh. Technol.*, vol. 63, no. 2, pp. 518–526, Feb. 2014.

[12] M. Arti, “Channel estimation and detection in hybrid satellite-terrestrial communication systems,” *IEEE Trans. Veh. Technol.*, 2015, http://ieeexplore.ieee.org/xpl/login.jsp?tp=&arnumber=7156170, to be published.

[13] M. Arti and M. Bhatnagar, “Beamforming and combining in hybrid satellite-terrestrial cooperative systems,” *IEEE Commun. Lett.*, vol. 18, no. 3, pp. 483–486, Mar. 2014.

[14] M. Arti and M. Bhatnagar, “Two-way mobile satellite relaying: A beamforming and combining based approach,” *IEEE Commun. Lett.*, vol. 18, no. 7, pp. 1187–1190, Jul. 2014.

[15] M. Arti, “Imperfect CSI based maximal ratio combining in shadowed-rician fading land mobile satellite channels,” in *Proc. 21st Nat. Conf. Commun. (NCC)*, Feb. 2015, pp. 1–6.

[16] M. Bhatnagar, “On the sum of correlated squared κ-μ shadowed random variables and its application to performance analysis of MRC,” *IEEE Trans. Veh. Technol.*, vol. 64, no. 6, pp. 2678–2684, Jun. 2015.

[17] J. F. Paris, “Outage probability in η-μ/η-μ and κ-μ/η-μ interference-limited scenarios,” *IEEE Trans. Commun.*, vol. 61, no. 1, pp. 335–343, Jan. 2013.

[18] D. da Costa and M. Yacoub, “Average channel capacity for generalized fading scenarios,” *IEEE Commun. Lett.*, vol. 11, no. 12, pp. 949–951, Dec. 2007.

[19] S. Kumar, G. Chandrasekaran, and S. Kalyani, “Analysis of outage probability and capacity for κ-μ/η-μ faded channel,” *IEEE Commun. Lett.*, vol. 19, no. 2, pp. 211–214, Feb. 2015.

[20] L. Hanzo, M. El-Hajjar, and O. Alamri, “Near-capacity wireless transceivers and cooperative communications in the MIMO era: Evolution of standards, waveform design, and future perspectives,” *Proc. IEEE*, vol. 99, no. 8, pp. 1343–1385, Aug. 2011.

[21] M. Bhatnagar and M. Arti, “On the closed-form performance analysis of maximal ratio combining in shadowed-rician fading LMS channels,” *IEEE Commun. Lett.*, vol. 18, no. 1, pp. 54–57, Jan. 2014.

[22] K. Gharaibeh, K. Gard, and M. Steer, “Accurate estimation of digital communication system metrics–SNR, EVM and ρ; in a nonlinear amplifier environment,” in *Proc. ARFTG Microw. Meas. Conf.*, Dec. 2004, pp. 41–44.

[23] R. Shafik, S. Rahman, and R. Islam, “On the extended relationships among EVM, BER and SNR as performance metrics,” in *Proc. Int. Conf. Elect. Comput. Eng. (ICECE)*, Dec. 2006, pp. 408–411.

[24] H. Mahmoud and H. Arslan, “Error vector magnitude to SNR conversion for nondata-aided receivers,” *IEEE Trans. Wireless Commun.*, vol. 8, no. 5, pp. 2694–2704, May 2009.

[25] N. Ermolova and O. Tirkkonen, “Bivariate η-μ fading distribution with application to analysis of diversity systems,” *IEEE Trans. Wireless Commun.*, vol. 10, no. 10, pp. 3158–3162, Oct. 2011.

[26] N. Y. Ermolova, “Moment generating functions of the generalized η-μ and κ-μ distributions and their applications to performance evaluations of communication systems,” *IEEE Commun. Lett.*, vol. 12, no. 7, pp. 502–504, Jul. 2008.

[27] K. Peppas, F. Lazarakis, A. Alexandridis, and K. Dangakis, “Error performance of digital modulation schemes with MRC diversity reception over η-μ fading channels,” *IEEE Trans. Wireless Commun.*, vol. 8, no. 10, pp. 4974–4980, Oct. 2009.

[28] N. Y. Ermolova and O. Tirkkonen, “Bivariate η-μ fading distribution with application to analysis of diversity systems,” *IEEE Trans. Wireless Commun.*, vol. 10, no. 10, pp. 3158–3162, Oct. 2011.

[29] S. Kalyani and R. Karthik, “The asymptotic distribution of maxima of independent and identically distributed sums of correlated or non-identical gamma random variables and its applications,” *IEEE Trans. Commun.*, vol. 60, no. 9, pp. 2747–2758, Sep. 2012.

[30] H. Exton, *Multiple Hypergeometric Functions and Applications*. New York, NY, USA: Halsted Press, Ellis Horwood, 1976.

[31] F. G. Tricomi and A. Erdlyi, “The asymptotic expansion of a ratio of gamma functions,” *Pac. J. Math.*, vol. 1, no. 1, pp. 133–142, 1951.

[32] N. M. Temme, “Large parameter cases of the gauss hypergeometric function,” *J. Comput. Appl. Math.*, vol. 153, no. 1, pp. 441–462, 2003.

[33] S. Kumar and S. Kalyani, “Coverage probability and rate for η-μ/κ-μ fading channels in interference-limited scenarios,” *IEEE Trans. Wireless Commun.*, vol. 14, no. 11, pp. 6082–6096, Nov. 2015.

Varghese Antony Thomas received the B.E. (Hons.) degree in electrical and electronics engineering from Birla Institute of Technology and Science, Pilani (Goa Campus), India, in 2010, and the M.Sc. degree in wireless communications and the Ph.D. degree from the University of Southampton, Southampton, U.K., in 2011 and 2015, respectively. He is a Research Associate with Georgia Institute of Technology, Atlanta, GA, USA. As a Ph.D. student, he worked with the Wireless Communications Research Group of the University of Southampton. His research interests include optical communications, optical-wireless integration, backhaul for MIMO, and radio over fiber systems. He was the recipient of several academic awards including the Commonwealth Scholarship of the Government of U.K. and Mayflower Scholarship of University of Southampton.

Suman Kumar received the B.Tech degree in electronics and communication engineering from the Future Institute of Engineering and Management, Kolkata, India, in 2010. He is currently pursuing the Ph.D. degree at the Department of Electrical Engineering, IIT Madras, Chennai, India.

His research interests include performance analysis of mobile broadband wireless networks including frequency reuse, HetNets, hypergeometric functions, and generalized fading models. He was the recipient of the Best Paper Award at ICWMC-2012 held at Venice, Italy.

Sheetal Kalyani received the B.E. degree in electronics and communication engineering from Sardar Patel University, Gujarat, India, in 2002, and the Ph.D. degree in electrical engineering from the Indian Institute of Technology (IIT) Madras, Chennai, India, in 2008. She was a Senior Research Engineer with the Centre of Excellence in Wireless Technology, Chennai, India, from 2008 to 2012. She is is currently an Assistant Professor with the Department of Electrical Engineering, IIT Madras.

Her research interests include HetNets, extreme value theory, hypergeometric functions, generalized fading models, and statistical learning algorithms for prediction in wireless networks.

Mohammed El-Hajjar received the B.Eng. degree in electrical engineering from the American University of Beirut, Lebanon, in 2004, and the M.Sc. degree in radio frequency communication systems and the Ph.D. degree in wireless communications from the University of Southampton, Southampton, U.K., in 2005 and 2008, respectively. Following the Ph.D., he joined Imagination Technologies as a Design Engineer, where he worked on designing and developing Imagination's multistandard communications platform, which resulted in three patents. Since January 2012, he has been a Lecturer with the Southampton Wireless Research Group, School of Electronics and Computer Science, University of Southampton, Southampton, U.K. He has authored a Wiley-IEEE book and more than 60 journal and international conference papers. His research interests include the development of intelligent communications systems including energy-efficient transceiver design, multifunctional MIMO, millimetre wave communications, and radio over fibre systems.

K. Giridhar received the B.Sc. degree in applied sciences from PSG College of Technology, Coimbatore, India, the M.E. degree in electrical communications from Indian Institute of Science, Bangalore, India, and the Ph.D. degree in electrical engineering from the University of California, Santa Barbara, Santa Barbara, CA, USA. Between 1989 and 1990, he was a Member of Research Staff with CRL, Bharat Electronics, Bangalore, India, and between 1993 and 1994, was a Research Affiliate in electrical engineering with Stanford University, Stanford, CA, USA. Since 1994, he has been with the Department of Electrical Engineering, IIT Madras (IITM), Chennai, India.

He serves as a Consultant to many Telecom & VLSI companies in India, and was on a Sabbatical from 2004 to 2005 with Beceem Communications. He has been a Visiting Faculty at Sri Sathya Sai Institute of Higher Learning, Prasanthi Nilayam, Anantapur, India, and Stanford University. His research interests include adaptive signal processing and wireless communications systems, with an emphasis on various transceiver algorithms, custom air-interface design for strategic applications, and performance analysis of mobile broadband wireless networks including HetNets.

He is a Member of the Telecommunications and Computer Networks (TeNeT) Group at IITM. He actively collaborates with the Center of Excellence in Wireless Technology on MIMO-OFDM broadband access research, resulting in several contributions to IEEE 802.16m, and currently on proposals to LTE-A and 5G forums.

Lajos Hanzo (M'91–&SM'92–F'04) received the degree in electronics in 1976 and the doctorate degree in 1983. During his 40-year career in telecommunications, he has held various research and academic posts in Hungary, Germany, and the U.K. Since 1986, he has been with the School of Electronics and Computer Science, University of Southampton, U.K., where he holds the chair in telecommunications. He has successfully supervised about 100 Ph.D. students, co-authored 20 John Wiley/IEEE Press books on mobile radio communications totalling in excess of 10,000 pages, published over 1500 research entries at IEEE Xplore, acted both as the TPC and the General Chair of IEEE conferences, presented keynote lectures, and has been awarded a number of distinctions. Currently, he is directing a 60-strong academic research team, working on a range of research projects in the field of wireless multimedia communications sponsored by industry, the Engineering, and Physical Sciences Research Council (EPSRC), U.K., the European Research Council's Advanced Fellow Grant, and the Royal Society's Wolfson Research Merit Award. His research is funded by the European Research Council's Senior Research Fellow Grant. Lajos has over 23,000 citations. He is an enthusiastic supporter of industrial and academic liaison and offers a range of industrial courses. He is a Fellow of Royal Academy of Engineering, the Institution of Engineering and Technology, the EURASIP, and DSc. He is also a Governor of the IEEE VTS. From 2008 to 2012, he was the Editor-in-Chief of the IEEE Press and also a Chaired Professor at Tsinghua University, Beijing, China. In 2009, he was awarded an Honorary Doctorate by the Technical University of Budapest, while in 2015 by the University of Edinburgh.